POLITECNICO DI TORINO



The wear effect of cliff in marine environment

Student: Kuang Yu (s327310)

Supervisors:

Prof. Monica Barbero

Prof. Maria Lia Napoli

Content

1. Introduction 6
1.1 Background 6
1.2 Research Problem 7
1.3 Research Aim and Objectives 9
1.4 Research Scope and Methodology 10
1.5 Thesis Structure 11
2. Literature Review 12
2.1 Introduction 12
2.2 Coastal Rock Cliffs as Geotechnical Systems 14
2.3 Marine processes and wear effect 17
3. The case study 23
3.1 Introduction 23
3.2 Site Location 24
3.3 Topography and Cliff Geometry 26
3.4 Geological Setting and Stratigraphy 26
3.5 Hydrogeological and rainfall conditions 29
3.6 Mechanical Properties 30
3.7 Data Quality and Uncertainty 33
4. Methodology and numerical modelling 33
4.1 General workflow 33
4.2 Introduction of Numerical Software and Analysis Type 34
4.3 Model Geometry and Domain Size 36
4.5 Mechanical Properties of the Materials 37
4.6 Scenario 1: Baseline condition 37
4.7 Scenario 2: Rainfall action without Weathering 38
4.8 Scenario 3: Rainfall Condition with Weathering 40
4.9 Scenario 4: with joints 43
5. Results 45
5.1 Introduction 45
5.2 Scenario 1 46

5.3 Scenario 2 47
5.4 Scenario 3 50
5.5 Scenario 4 53
6. Discussion and Conclusion 56
Reference list: 62

List of figures

Figure 1: Schematic representation of the failure mechanisms 16
Figure 2: Mechanism of toppling failure 16
Figure 3: Schematic representation of marine erosion (Miccadei et al.,2019, modified) 17
Figure 4: Location of the Mimi study site on the North Taranaki coast, New Zealand (coordinate: -38.954948,174.444283; ZTM2000) 25
Figure 5: Aerial view of the Mimi coastal cliff(source: Google Earth) 25
Figure 6: Comparison of the cliff profiles surveyed on 15 April 2023 and 14 December 2023 26
Figure 7: Simplified stratigraphic profile of the Mimi cliff 27
Figure 8: Representative discontinuities observed in the Mount Messenger Formation at Mimi. 28
Figure 9: Orientation of the main discontinuity sets characterizing the Mimi cliff face 28
Figure 10: Weekly rainfall data of interested region 29
Figure 11: GSI index by Hook & Brown (2000) 31
Figure 12: Geometry of numerical cliff model (before excavation) 36
Figure 13: Numerical model for scenario 2 (including water boundary condition) 40
Figure 14: The geological layout of materials for scenario 3 42
Figure 15: Numerical model for scenario 4 (top: global model; bottom: zoomed jointed area) ... 45
Figure 16: Major principal stress (Sigma 1) distribution at the critical SRF of 1.08 for Scenario 1. 46
Figure 17: Maximum shear plastic strain distribution at the critical SRF of 1.08 for Scenario 1 47
Figure 18: Distribution of yielded elements at the critical SRF of 1.08 for Scenario 1 47
Figure 19: Total head distribution and groundwater flow directions at the critical SRF of 0.62 for Scenario 2 48
Figure 20: Distribution of yielded elements at the critical SRF of 0.62 for Scenario 2 49
Figure 21: Maximum shear plastic strain distribution at the critical SRF of 0.62 for Scenario 49
Figure 22: Total head distribution and groundwater flow directions under the weekly averaged rainfall condition at the critical SRF of 0.49 50
Figure 23: Distribution of yielded elements under the weekly averaged rainfall condition at the critical SRF of 0.49 50
Figure 24: Maximum shear plastic strain distribution under the weekly averaged rainfall condition at the critical SRF of 0.49 51
Figure 25: Total head distribution and groundwater flow directions under the daily rainfall condition at the critical SRF of 0.50 51
Figure 26: Distribution of yielded elements under the daily rainfall condition at the critical SRF of 0.50 52
Figure 27: Maximum shear plastic strain distribution under the daily rainfall condition at the critical SRF of 0.50 52
Figure 28: Maximum shear plastic strain distribution under the dry condition for Scenario 4 53

Figure 29: Distribution of yielded joints within the jointed Mount Messenger Formation under the dry condition 53
Figure 30: normal displacement along yielded joints under the dry condition (scenario 4)..... 54
Figure 31: shear displacement along yielded joints under the dry condition (scenario 4) 54
Figure 32: Maximum shear plastic strain distribution under the weekly averaged rainfall condition for Scenario 4. 55
Figure 33: Normal displacement among yielded joints under the weekly averaged rainfall condition..... 55
Figure 34: Shear displacement among yielded joints under the weekly averaged rainfall condition 56

List of tables:

Table 1: discontinuity sets for the Mount Messenger Formation *29*
Table 2: Summary of Mount Messenger formation *30*
Table 3: Main properties of Mount Messenger Formation *32*
Table 4: The main material strength parameters of Rapanui formation *32*
Table 5: Material properties for scenario 1 ..... *38*
Table 6: hydraulic conductivities for 2 formations in scenario 2 ..... *40*
Table 7: Main mechanical properties of materials involved in scenario 3 ..... *42*

1. Introduction

1.1 Background

Coastal cliffs are naturally dynamic landforms that are continuously modified by the interaction between geological conditions and environmental processes. Their long-term evolution is generally controlled by a combination of marine and subaerial processes, while the relative importance of these processes varies depending on cliff geometry, lithology, rock mass structure, and local environmental conditions (Sunamura, 1992; Young *et al.,* 2009; Earlie *et al.,* 2018).

Cliff instability is rarely controlled by a single mechanism. The upper part of a cliff is commonly influenced by rainfall infiltration, groundwater movement, and subaerial weathering, whereas the lower part is more directly exposed to wave attack and marine erosion. Field monitoring of coastal cliffs has shown that rainfall and groundwater processes can trigger or accelerate upper-cliff failures, while wave action contributes strongly to erosion and weakening near the cliff toe (Young et *al*., 2009; Young *et al*., 2021). The interaction between these processes can therefore produce progressive weakening followed by episodic mass failure.

Rainfall infiltration may alter the hydraulic conditions within a cliff through changes in water content and pore-water pressure, consequently affecting effective stress and slope stability. At the same time, prolonged exposure to water and repeated wetting and drying can progressively degrade rock material. Experimental studies have demonstrated that water saturation and repeated freshwater or seawater weathering cycles can significantly reduce rock strength and stiffness, although the magnitude of degradation depends strongly on lithology and rock structure (Duperret *et al*., 2005).

The cliff is influenced in a different way in marine environment. Wave energy reaching the cliff toe can cause abrasion, hydraulic action, and progressive removal or weakening of material, while extreme wave conditions can account for a substantial proportion of short-term cliff erosion (Earlie *et al*., 2018). Continued erosion or degradation of the lower cliff can reduce toe support and increase the susceptibility of the overlying slope to instability. Coastal cliff evolution should therefore be considered as the result of interacting geological, hydrological, weathering, and marine processes rather than the response to one isolated forcing mechanism (Young *et al*., 2009; Genchi *et al*., 2025).

The Taranaki coastline of New Zealand, the case study analyzed in this thesis, provides a suitable setting for investigating these interactions. The study area contains sedimentary units with different lithological and mechanical characteristics, including exposures of the Mount Messenger Formation along the North Taranaki coast. The

formation is widely exposed in coastal cliffs and consists of sedimentary successions whose contrasting material and structural characteristics provide an appropriate geological setting for investigating rock mass behavior and cliff instability.

Understanding the relative influence of these processes from field observations alone is difficult because rainfall, groundwater, weathering, wave exposure, and geological features act simultaneously and over different time scales. Numerical modelling provides a useful means of separating these effects by progressively introducing individual factors and comparing the resulting changes in stress, deformation, pore-water pressure, and slope stability.

1.2 Research Problem

Conventional slope stability assessment often represents a rock slope using fixed mechanical properties and simplified groundwater conditions. Such an approach can provide a useful indication of overall stability, but it may not adequately represent a coastal cliff where material properties and hydraulic conditions vary both spatially and temporally.

For the cliff investigated in this study, several issues are particularly important. First, the rock mass contains discontinuities and cannot always be represented adequately as a completely homogeneous intact material. Depending on the geological unit and the purpose of the analysis, the influence of discontinuities may need to be represented either explicitly or through equivalent rock mass properties. The selection of an appropriate rock mass geotechnical model therefore has a direct influence on the predicted deformation and failure behavior.

A further difficulty is the limited availability of site-specific geotechnical data. Although the general stratigraphy, cliff geometry, weathering features, and visible patterns of retreat can be identified from field observations and available geological information, detailed mechanical properties for the individual materials are not available for all units and weathering conditions. In particular, due to the lack of comprehensive site-based laboratory testing, parameters such as Young’s modulus, cohesion, tensile strength, friction angle, and the extent of strength reduction caused by weathering or marine exposure cannot be reliably determined for all involved material.

This data limitation also introduces considerable uncertainty into the numerical model. Rather than assigning a single set of assumed mechanical properties and treating them as exact values, the model development therefore follows an iterative process. Initial material parameters are selected from available geological information, published data, and reasonable engineering ranges. Numerical results are then compared with

observable characteristics of the actual cliff, including the location and approximate extent of retreat, surface deformation, weathered zones, and instability visible in field photographs. Where the numerical response is clearly inconsistent with the observed behavior, the relevant material parameters are progressively adjusted within physically reasonable ranges.

In this sense, the numerical modelling is used not only as a predictive tool but also as a form of engineering back-analysis. The aim is not to determine a unique set of material properties, which would not be possible with the available field data, but to identify parameter combinations that can reproduce the main characteristics of the observed cliff behavior. This approach also allows the relative sensitivity of the model to changes in strength and stiffness to be examined. The final adopted properties should therefore be interpreted as representative modelling parameters rather than direct measurements of the in-situ rock mass.

This limitation is particularly important when weathering is considered. Weathering is concentrated mainly near exposed surfaces rather than occurring uniformly throughout the slope, and the properties of this near-surface material may differ substantially from those of the less weathered rock behind it. Therefore, the depth and mechanical condition of the weathered zone need to be inferred partly from visible field evidence and the observed pattern of cliff retreat. Ignoring this spatial variation would result in an overly simplified representation of the actual cliff.

Rainfall conditions introduce an additional source of complexity. Rainfall varies significantly over time, and the use of a constant or averaged rainfall condition may reproduce the general hydraulic loading applied to the slope but does not necessarily represent short-term variations in rainfall intensity. These variations can influence the development and dissipation of pore-water pressure and consequently alter the mechanical response of the cliff. It is therefore necessary to examine whether the temporal resolution of rainfall input has a meaningful effect on the predicted stability.

The lower part of the coastal cliff presents a further modelling challenge because it experiences environmental conditions that differ from those affecting the upper slope. Repeated wave exposure, wetting and drying, and associated marine weathering can lead to greater deterioration of the material close to the cliff toe. However, the degree of mechanical degradation caused by these processes is also difficult to quantify directly because site-specific long-term laboratory and field measurements are unavailable. The degraded material properties adopted in this part of the model therefore need to be constrained using published experimental evidence, field observations, and the resulting numerical behavior.

These uncertainties mean that the numerical model should not be interpreted as an exact reconstruction of the cliff. Instead, it represents a mechanically reasonable approximation developed from the available evidence. The main value of the modelling lies in examining how the predicted cliff behavior changes when different geological and environmental factors are introduced progressively, rather than in claiming an exact prediction of the timing or magnitude of future cliff failure.

The processes considered in this study are also strongly interconnected. Rock mass structure influences the way deformation develops, rainfall modifies hydraulic conditions, weathering reduces the resistance of near-surface materials, and degradation of the lower cliff can reduce support to the overlying slope. A model that considers only one of these influences may therefore fail to reproduce the range of instability observed in the field.

The central research problem addressed by this study is consequently how a coastal cliff with limited site-specific geotechnical data can be represented in a physically reasonable numerical model, and how the progressive inclusion of rainfall, weathering, rock mass conditions, and wave-related material degradation changes the predicted deformation and stability of the cliff.

1.3 Research Aim and Objectives

The main aim of this research is to investigate the influence of weathering on the retreat and instability of a coastal cliff through numerical modelling, with the reference to the Taranaki coastline in New Zealand. The study is based on an observed period of cliff retreat, which provides an important reference for understanding the actual behavior of the slope and for evaluating the numerical results.

The research first seeks to develop a representative two-dimensional model of the cliff using the available information on cliff geometry, stratigraphy, rock mass conditions, field photographs, and the observed pattern of retreat. Because detailed site-specific mechanical properties are limited, the numerical model is developed progressively, with material parameters adjusted within reasonable ranges by comparing the simulated response with the behavior visible in the field. In this way, the observed retreat is used not only as a final point of comparison, but also as an important constraint during model development.

A major focus of the study is to examine whether the observed retreat can be reasonably explained by the original geological and mechanical conditions of the cliff, or whether degradation caused by weathering needs to be introduced to reproduce a more realistic response. Weathering is therefore incorporated progressively into the model through

changes in the mechanical properties of the near-surface rock mass. Particular attention is given to the development of displacement, strain, instability, and the spatial extent of deformation, and these results are compared with the location and approximate depth of retreat observed in the field.

Rainfall is also considered because it can modify the hydraulic condition of the cliff and may contribute to the development of instability. Both actual daily rainfall and weekly averaged rainfall are applied in the numerical analyses in order to examine whether different temporal representations of rainfall produce meaningful differences in pore-water pressure and mechanical response. This comparison also provides an indication of whether simplified rainfall inputs are sufficient for representing the general behavior of the cliff.

In addition, the lower part of the cliff is examined separately because it is exposed to stronger marine influence. The possible degradation of mechanical properties associated with repeated wave exposure and marine weathering is incorporated into the numerical model to investigate how weakening near the cliff toe may contribute to local instability and continued retreat.

Through comparison of the different numerical results, the study ultimately aims to determine how important weathering is in explaining the observed cliff retreat, how its influence interacts with rainfall and marine-related degradation, and whether the progressively developed numerical model can reproduce the main spatial characteristics of the instability observed at the study site. The intention is not to reproduce every individual failure event exactly, but to establish a mechanically reasonable explanation for the observed retreat and to identify the processes that are most relevant to its development.

1.4 Research Scope and Methodology

This research focuses on a representative two-dimensional section of a coastal cliff in Taranaki. The study does not attempt to reproduce the complete long-term geomorphological evolution of the coastline. Instead, it investigates the mechanical response of the selected cliff section under a series of progressively more realistic geological and environmental conditions.

The numerical analysis is carried out using the Finite Element Method, implemented in the code RS2 by Rocscience. The cliff geometry, geological units, material properties, weathering conditions, and hydraulic conditions are established using the geological and field information available for the study site. Different models are used to represent the rock mass according to the characteristics of the individual geological units and the

purpose of each modelling scenario.

A series of numerical scenarios is developed so that the influence of individual processes can be identified more clearly. A relatively simple condition is first used as a reference case. Additional factors are then introduced progressively, including rainfall infiltration and weathering. Rainfall is represented using both actual daily rainfall and weekly averaged rainfall to examine whether temporal averaging changes the predicted hydraulic and mechanical response of the cliff.

The modelling is subsequently extended to consider the lower part of the cliff in greater detail. In this region, marine exposure is represented through degradation of the relevant mechanical properties. Discontinuities are also incorporated where necessary to better represent the rock mass behavior while maintaining a practical numerical model size.

The results are evaluated mainly in terms of global factor of safety, displacements, strain, pore-water pressure, and the spatial development of unstable or highly deformed zones. Comparison between scenarios is then used to determine how progressively incorporating environmental degradation changes the predicted behavior of the cliff.

Processes such as individual wave impacts, direct mechanical removal of material during a storm, and fully coupled long-term geomorphological retreat are not simulated explicitly. Instead, their effects are represented through changes in material condition and mechanical properties.

1.5 Thesis Structure

This thesis is organized into six chapters.

Chapter 1 introduces the background of coastal cliff instability, defines the research problem, and presents the aim, objectives, scope, and significance of the study.

Chapter 2 reviews previous research related to coastal cliff instability and retreat. It discusses the main geological and environmental controls on cliff behaviour, including rock mass properties, discontinuities, rainfall and groundwater, weathering, wave action, abrasion and toe erosion, wetting and drying cycles, and other degradation processes. Previous applications of numerical modelling to coastal slope stability are also considered.

Chapter 3 presents the case study and establishes the geological and engineering basis for the numerical modelling. It describes the location and regional setting of the study site, cliff geometry, geological units, material conditions, weathering characteristics, rainfall information, marine environment, and relevant mechanical and hydraulic properties.

Chapter 4 describes the development of the numerical models in RS2. It presents the model geometry, material models, rock mass representation, discontinuities, boundary conditions, hydraulic conditions, weathered zones, rainfall inputs, and the treatment of material degradation associated with wave exposure. The numerical scenarios used throughout the study are also defined in this chapter.

Chapter 5 presents the results of the numerical analyses. The predicted factor of safety, pore-water pressure, displacement, strain, and spatial patterns of instability are compared between the different modelling scenarios, including the effects of rainfall, weathering, rock mass representation, and lower-cliff material degradation.

Chapter 6 discusses the numerical results in relation to the physical behavior of the coastal cliff. The relative importance of the different controlling factors is evaluated, and the implications of the modelling results for cliff retreat and instability are considered. The limitations of the numerical approach and the assumptions adopted in the study are also discussed.

2. Literature Review

2.1 Introduction

Coastal rock cliffs are a common type of natural rock slope located at the boundary between land and sea. From a geotechnical perspective, the stability of a coastal cliff is controlled by several interacting factors, including geological conditions, rock-mass properties, groundwater conditions and environmental actions. Therefore, a coastal cliff should not only be considered as a geomorphological feature, but also as a complex geotechnical system.

The first important factor controlling cliff stability is the geological condition of the slope. Coastal cliffs commonly contain different lithological units, bedding planes, joints, weak layers and weathered zones. These features can significantly influence the strength, stiffness and deformation behavior of the rock mass. In particular, the strength of intact rock obtained from laboratory testing cannot directly represent the strength of the entire rock mass in the field. This is because natural rock masses usually contain discontinuities and geological defects, which can reduce their overall strength and change the possible failure mechanism.

In addition to geological conditions, coastal cliffs are continuously affected by environmental processes. The upper part of the cliff is mainly influenced by processes such as rainfall infiltration, wetting and drying, runout weathering and wind weathering. On the other hand, the lower part of the cliff is additionally exposed to marine processes,

including wave action, seawater wetting, abrasion and erosion. Although these processes act in different ways, they can gradually change either the cliff geometry or the engineering properties of the rock mass. As a result, cliff instability may not be caused by a single event. Instead, it may develop progressively after a long period of material degradation and stress redistribution.

Hydrological conditions are another important factor affecting coastal cliff stability. Rainfall can infiltrate into the slope through the rock matrix, weathered materials, bedding planes and open discontinuities. This infiltration can change the groundwater condition and pore-water pressure within the slope. In fractured rock masses, water flow may be highly non-uniform because joints and cracks can act as preferential flow paths. At the same time, repeated water infiltration can contribute to further deterioration of weak or weathered materials (Duperret *et al.*, 2005).

Therefore, the stability of a coastal rock cliff can be considered as the result of four main interacting components: geological structure, hydraulic conditions, mechanical properties and environmental wear processes. Geological heterogeneity determines the initial distribution of strength and permeability. Discontinuities control both mechanical weakness and possible water-flow paths. Rainfall changes the hydraulic condition of the slope, while long-term marine and atmospheric exposure may progressively reduce the quality of the rock mass. These changes can finally influence effective stress, deformation behavior and shear resistance, and therefore affect the overall stability of the slope.

It is also important to point out that these processes do not affect the entire cliff in the same way. Different parts of a coastal cliff may be controlled by different mechanisms. For example, the upper slope may be more sensitive to rainfall infiltration and weathering, whereas the lower cliff may experience stronger marine influence. Because of these complexities, the analysis of the stability of cliff may be conducted by numerical methods. Previous studies have shown that combining geological investigation with numerical modelling can provide a more realistic interpretation of instability coastal cliffs (Fazio *et al*., 2019; Napoli *et al.*, 2024). However, numerical modelling of coastal cliffs requires several important simplifications and assumptions. The natural cliff must first be converted into an engineering model by defining the major geological units, mechanical properties, hydraulic properties, discontinuities and boundary conditions. In addition, decisions are required regarding whether discontinuities should be represented indirectly through equivalent rock-mass properties or explicitly as individual structural features. These modelling choices directly affect which physical processes can be reproduced in the numerical analysis.

2.2 Coastal Rock Cliffs as Geotechnical Systems

Coastal rock cliffs can be regarded as natural rock slopes whose stability is controlled by the interaction between geological structure, slope geometry and environmental conditions. From a geotechnical perspective, the main components of a coastal cliff include the cliff face, cliff top, cliff toe, weathered zones and the internal discontinuity network. These components have different functions and therefore should not be treated as a uniform rock mass.

The cliff face represents the main exposed free surface of the slope, while the cliff top is an important zone for rainfall infiltration. The cliff toe provides support to the overlying rock mass and is also the part most directly influenced by marine action. Weathered zones usually show lower mechanical quality than less altered rock, while discontinuities such as joints and bedding planes can reduce rock-mass strength and provide preferential pathways for water flow. Therefore, the behavior of a coastal cliff depends not only on its external geometry but also on the internal geological condition of the rock mass.

2.2.1 Geological and Geomorphological Setting

Steep cliff faces provide limited lateral support and may promote instability when unfavorably oriented discontinuities are present. Local erosion or rockfall can further modify the slope profile and cause stress redistribution within the remaining rock mass, and these repeated local failures can progressively contribute to long-term cliff retreat (Rosser *et al.*, 2013)

The cliff toe is particularly important because it provides mechanical support to the upper part of the slope. Marine erosion or degradation at the toe may reduce this support and increase the potential for instability. Furthermore, accumulated fallen rock blocks or beach sediments may temporarily protect the toe from direct wave actions (López-Fernández *et al.*, 2022).

The cliff top is important from a hydraulic perspective because rainfall can infiltrate through the ground surface and migrate towards the slope. Open joints and tension cracks near the crest may further increase infiltration and at the same time reduce mechanical continuity.

Weathered and degraded zones also form an important part of the cliff system. Rock close to the exposed surface may have lower strength and stiffness than less weathered material at depth. Therefore, spatial variations in weathering condition should be considered when interpreting the mechanical behavior of coastal rock slopes.

2.2.2 Rock-Mass Structure

Natural rock masses are rarely continuous and homogeneous. Their behavior is influenced by lithology, bedding, joints, faults, weak layers and different degrees of weathering. Therefore, the stability of a coastal cliff, as for almost all rock masses, cannot be assessed only from the strength of intact rock specimens.

Many previous studies show that discontinuity geometry is a major control on instability in rocky coastal cliffs. Bedding, joints and faults can control both deformation and failure. Their influence depends mainly on orientation, spacing, persistence and shear strength. For example, discontinuities with similar dip direction as the cliff face may promote sliding, or toppling, depending on their dip.

In addition, weak layers may also control the overall slope behavior. A relatively weak material can concentrate deformation even when it is surrounded by stronger rock. At the same time, stronger but jointed rock may still develop local joint displacement or yielding. This means that different parts of the same slope can exhibit different mechanical responses.

2.2.3 Common Failure Mechanisms

The failure mechanism of a coastal rock cliff is mainly controlled by discontinuity characteristics, material strength, groundwater conditions and slope geometry. Common failure modes include translational sliding, wedge failure, toppling, rockfall and composite failure.

Translational sliding may occur when a persistent bedding plane or discontinuity and cliff face have similar dip direction. In highly fractured or weak rock masses, failure may develop as a rotational or composite mechanisms, involving both weak materials and discontinuities. Wedges failure develops through the intersection of multiple discontinuities and is therefore strongly three-dimensional. The schematic representation of the mechanism of planar sliding, rotational sliding and wedge failure are shown in figure 1.

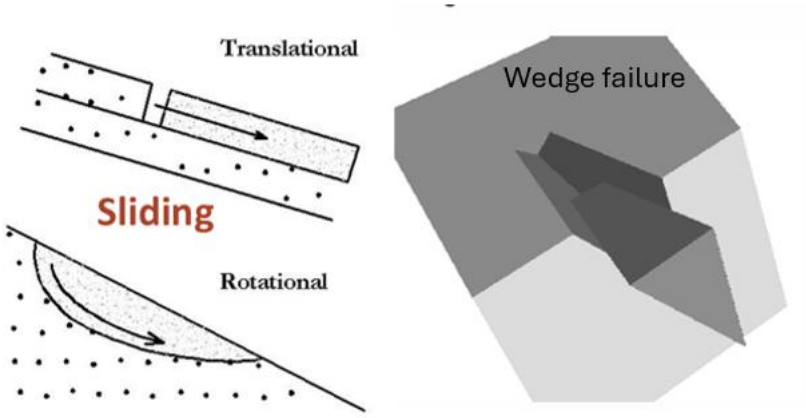


Figure 1: Schematic representation of the failure mechanisms

Toppling generally develops where steeply dipping discontinuities divide the rock mass into blocks or columns that can rotate in the direction of the free face. Rockfall and block detachment may occur when joints isolate individual blocks and progressive weathering, rainfall or stress redistribution reduces their stability.

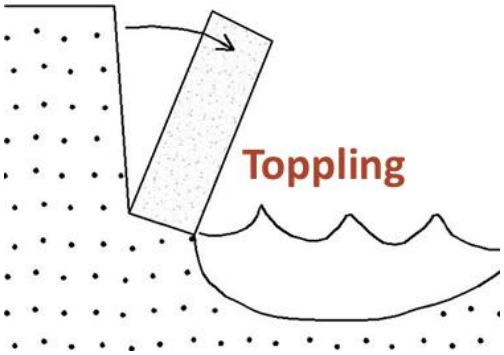


Figure 2: Mechanism of toppling failure

Marine erosion can also contribute to instability through toe undercutting. Removal or weakening of material at the cliff base reduces support and causes stress redistribution, which may eventually lead to gravity-driven collapse (figure 3). Rainfall and groundwater can further promote these mechanisms by increasing pore-water pressure, reducing effective stress and weakening discontinuities or weathered material.

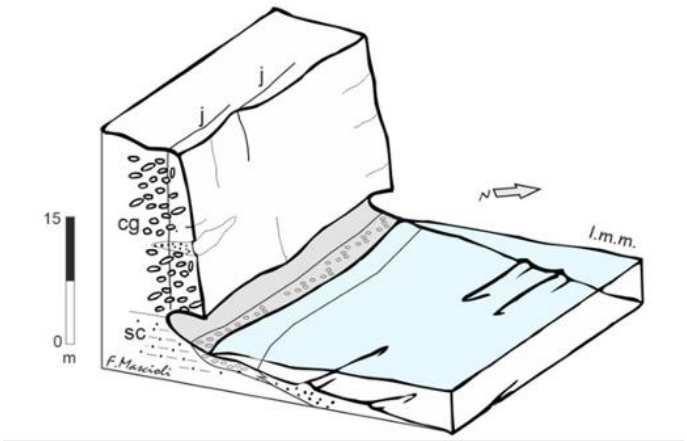


Figure 3: Schematic representation of marine erosion (Miccadei *et al*.,2019, modified)

Importantly, coastal cliff failure may develop progressively. Initial deformation may involve small joint displacements, local yielding or minor rockfalls before a larger failure mechanism develops. Therefore, slope stability should not always be interpreted only through a global factor of safety. In jointed or heterogeneous rock masses, local deformation, yielded zones and joint displacement may also provide important information on the development of instability.

2.3 Marine processes and wear effect

Marine processes are one of the main factors that distinguish coastal rock cliffs from conventional inland rock slopes. In addition to gravitational loading, rainfall and groundwater, the lower part of a coastal cliff is continuously affected by waves, tides, seawater and sediment movement. These processes can directly remove material from the cliff, but they can also gradually change the physical and mechanical properties of the remaining rock mass. Therefore, the long-term influence of the marine environment should not only be considered in terms of visible cliff erosion or retreat. From a geotechnical perspective, the progressive degradation of rock strength, stiffness and discontinuity conditions is also important because these changes may reduce slope resistance before large-scale failure occurs.

Previous studies have shown that the development of rocky coasts is controlled by the combined effects of wave action, material resistance, weathering and geological structure rather than by a single process (Trenhaile, 2002; Naylor *et al*., 2010; Sunamura, 2015). Therefore, this section reviews the main environmental processes that can contribute to rock-mass degradation. The wave action, abrasion and toe undercutting, wetting–drying cycles, salt crystallization and other secondary weathering processes will be discussed.

2.3.1 Mechanical Effects of Wave Action

Wave action is one of the main sources of mechanical energy acting on the lower part of coastal cliffs (Shen *et al.*, 2024). When waves reach a steep cliff face, part of their energy is transferred to the rock through water pressure and impact. The magnitude of this loading depends on several factors, including wave height, breaking conditions, water level, cliff geometry and the condition of the foreshore. Therefore, wave loading is highly variable in both space and time.

In general, wave action can influence coastal rock cliffs through two related mechanisms. The first is short-duration wave impact, which may produce locally high pressures on the exposed cliff surface. The second is repeated cyclic loading, in which successive waves cause small but repeated deformation of the rock mass. Although a single wave may not generate sufficient stress to cause immediate failure, a very large number of loading cycles can progressively influence the mechanical condition of the cliff.

The repeated nature of wave action is particularly important from a rock-mechanics perspective. Rock fatigue refers to progressive damage caused by repeated loading at stress levels that may be lower than the strength required to produce failure under a single monotonic loading event. Under cyclic loading, small irreversible strains can accumulate and existing microcracks can progressively grow. As the number of loading cycles increases, the damaged region may expand until macroscopic cracking or failure occurs.

Direct field evidence of this behaviors was provided by Adams *et al.* (2005), who monitored wave-induced ground motion in sea cliffs using near-coastal seismometers. Their results showed that wave loading caused measurable cyclical flexing of the cliff, with estimated longitudinal and shear strains of approximately 0.5–4 microstrain during individual wave-loading cycles. The authors estimated that such flexing could occur approximately three million times per year at the monitored site and therefore suggested that repeated wave loading has the potential to contribute to rock fatigue. Lim *et al.* (2011) also demonstrated that tidal conditions and wave impacts produce measurable ground motion in coastal rock cliffs, further supporting the concept that marine forcing can be transmitted into the rock mass rather than acting only on the exposed surface.

The effect of cyclic loading has also been investigated for rock types with different mechanical characteristics. Geranmayeh Vaneghi *et al.* (2018) tested sandstone and granodiorite under uniaxial cyclic compression and found that increasing loading amplitude resulted in shorter fatigue life and greater strength degradation. Importantly, the two rock types did not show the same degradation response, demonstrating that fatigue behavior is strongly dependent on lithology and rock structure.

The development of fatigue damage is generally associated with progressive microcracking. During repeated loading and unloading, pre-existing cracks may repeatedly open, close or slide (Yang *et al.*, 2025). Small irreversible deformations can accumulate, and new cracks may develop around existing defects and grain boundaries. With continued cycling, crack density and connectivity may increase, leading to a progressive reduction in effective material integrity.

Consequently, the mechanical influence of repeated wave loading can be represented conceptually as: cyclic stress and strain within the cliff, progressive microcrack initiation and propagation, fatigue damage and accumulated deformation, reduction in effective strength and stiffness.

2.3.2 Abrasion, Scour and Toe Undercutting

In addition to direct wave action, sediment transported by waves can contribute to coastal rock erosion. Sand, gravel, cobbles and fallen rock fragments may strike or rub against the cliff toe and shore platform. These materials can therefore act as abrasive tools and gradually remove weakened rock from exposed surfaces.

The efficiency of abrasion depends on both wave energy and sediment availability. A limited amount of mobile sediment may increase erosion because particles repeatedly impact the rock surface. However, if a thick layer of sediment or large rock blocks accumulates at the cliff toe, it may protect the cliff from direct wave attack (Sunamura, 2015). Therefore, sediment can either increase or reduce marine erosion depending on its quantity, size and mobility (Crouvi *et al.*, 2026).

Continued abrasion and erosion at the cliff base may lead to toe recession and undercutting. Over time, a notch or overhanging profile may develop. This process is important because it changes both the cliff geometry and the support condition of the overlying rock mass. Experimental and field studies have shown that wave-driven abrasion can progressively deepen basal notches and that notch development is strongly influenced by wave energy and sediment movement (Shen *et al.,* 2024; Barlow, 2025).

Firstly, the direct removal of material changes the external shape of the cliff. Secondly, the loss of support at the toe causes stress redistribution in the overlying rock mass. As undercutting increases, tensile stress may develop near the rear of the overhang, while stress concentration may occur around the remaining supporting material. Eventually, the cliff may fail through tensile cracking, sliding, rotation or a combination of these mechanisms (Napoli *et al.*, 2024).

The influence of undercutting also depends on geological structure. If discontinuities

already isolate a potential block, a relatively small amount of toe erosion may be sufficient to reduce its stability. In contrast, a massive and strong rock mass may tolerate greater undercutting before failure occurs.

2.3.3 Wetting–Drying cycles

Coastal rock cliffs are repeatedly subjected to changes in moisture condition due to rainfall, seawater, tidal variation and evaporation. Therefore, the exposed rock mass may experience repeated wetting–drying cycles. This repeated change in moisture condition is important because it can cause progressive deterioration of rock strength, stiffness and internal structure.

According to previous studies, during the wetting stage, water enters pores, microcracks and discontinuities within the rock. This may weaken cementation between mineral grains, reduce frictional resistance and cause swelling of hydrophilic clay minerals. During subsequent drying, water is removed and the rock may experience shrinkage and differential deformation. Repetition of these expansion–contraction processes can gradually enlarge existing pores and microcracks and weaken the internal structure of the material (Guo *et al.*, 2021; Huang *et al.*, 2018; Hua *et al.*, 2015; Zhao *et al.*, 2016).

Laboratory studies have demonstrated that wetting–drying cycles can significantly affect the mechanical properties of sedimentary rocks. Huang *et al.* (2018) investigated both sandstone and mudstone and found that uniaxial compressive strength and elastic modulus decreased with increasing numbers of wetting–drying cycles. This result is particularly relevant to weak sedimentary rock because it shows that repeated environmental exposure can affect both the resistance to failure and the deformation behavior of the material.

The effect is also evident in tensile and fracture behaviors. *Hua et al.* (2015) showed that repeated wetting and drying reduced the fracture toughness of sandstone, indicating that progressively weathered rock becomes less resistant to crack propagation. Guo *et al.* (2021) further investigated clay-bearing sandstone subjected to up to 40 wetting–drying cycles. Their experiments showed reductions in tensile strength of approximately 24–60%, together with decreasing stiffness and increasing ductility. Microstructural observations showed increasing intergranular cracking, greater pore development and deterioration of cementation as the number of cycles increased. Importantly, the magnitude of weakening was closely related to clay-mineral content.

An important observation from experimental studies is that degradation is generally non-linear. The first several wetting–drying cycles may produce relatively large changes, while the additional effect of later cycles can gradually decrease. For example,

Guo *et al.* (2021) found that the influence of each additional cycle on tensile-strength reduction became progressively smaller as cycling continued. Therefore, it is not appropriate to assume that rock strength decreases by a constant amount during every wetting–drying cycle.

These changes are important for coastal slope stability. A reduction in UCS or tensile strength decreases the resistance of the rock to failure, while a reduction in Young's modulus increases deformation under the same stress condition. At the same time, the development and connection of microcracks may modify permeability and allow water to penetrate further into the rock mass, creating a possible interaction between mechanical degradation and subsequent rainfall infiltration.

However, the magnitude of wetting–drying degradation varies considerably between rock types. In particular, clay-bearing and weakly cemented sedimentary rocks generally show greater sensitivity than rocks containing limited water-sensitive minerals. Zhao *et al*. (2017), for example, showed that sandstone with low clay-mineral content did not necessarily experience the same level of permanent tensile-strength degradation under repeated cycling as more clay-rich sandstone. Therefore, degradation parameters used in numerical modelling should be selected according to the lithology and available experimental evidence rather than applying a single reduction factor to all materials.

In summary, wetting–drying cycles can produce progressive and cumulative deterioration of coastal rock through repeated moisture-induced expansion, contraction, microcracking and weakening of mineral bonding. Experimental studies show corresponding reductions in compressive strength, tensile strength, fracture toughness and stiffness, with the magnitude of degradation strongly controlled by mineral composition and particularly clay content. These effects are therefore an important component of long-term rock-mass degradation in coastal environments.

2.3.4 Salt crystallization

Salt crystallization is an important weathering process in coastal rock environments because seawater and sea spray continuously introduce dissolved salts into pores, fractures and discontinuities. Sodium chloride (NaCl) is the dominant salt derived from seawater, although sulfate and magnesium salts may also occur depending on the local mineralogical and environmental conditions. During periods of wetting, saline water can penetrate into the pore network through capillary action. When the rock subsequently dries, evaporation increases the concentration of the pore solution and eventually causes salt precipitation. Repetition of this process can gradually damage

the internal structure of the rock mass. Reviews of salt weathering have identified crystallization within confined pore spaces as one of the principal mechanisms responsible for salt-induced deterioration of porous rock materials.

The main mechanism responsible for mechanical damage is crystallization pressure. When a saline solution becomes supersaturated, crystals begin to form and grow within the available pore space. If sufficient space is available, crystallization may occur without causing significant damage. However, when crystal growth is confined by the pore walls, pressure can be transferred to the surrounding rock matrix. Steiger (2005) demonstrated that crystallization pressure is closely related to the degree of supersaturation and the properties of the salt system. In general, greater supersaturation can generate higher crystallization pressures.

Whether salt precipitation causes significant mechanical damage also depends on where crystallization occurs. If evaporation is relatively slow compared with the supply of saline solution, salts may crystallize mainly at the external surface and form visible efflorescence. In contrast, when evaporation is sufficiently rapid, crystallization can occur within the pore network as sub-efflorescence. This internal crystallization is generally more damaging because crystal growth occurs under confinement and can generate stresses directly within the rock structure (Scrivano and Gaggero, 2020).

The resulting deterioration commonly begins at the microscopic scale. Repeated crystallization can initiate or enlarge microcracks, weaken grain contacts and promote granular disintegration. With continued cycling, individual cracks may become connected, leading to increased porosity, surface scaling and eventual loss of material. Therefore, salt weathering can progressively change the rock from a relatively intact material into a more fractured and mechanically weaker medium before large-scale erosion becomes visible.

2.3.5 Chemical, Thermal and Biological Effects

In addition to mechanical wave action, moisture changes and salt crystallization, other processes may also contribute to coastal rock degradation. These include chemical alteration, thermal effects, freeze–thaw processes and biological activity. However, their importance depends strongly on rock type and local environmental conditions.

Chemical weathering can be important in rocks containing soluble minerals or weak cementing materials. For example, carbonate rocks may experience dissolution, while cementing minerals in sandstone or mudstone may gradually alter under repeated exposure to water. Over long periods, these processes can reduce bonding between mineral grains and increase the susceptibility of the rock to mechanical erosion.

Thermal expansion and contraction can also contribute to microcracking. Different minerals have different thermal properties, and repeated temperature changes may generate differential strain between grains. When combined with repeated moisture changes, this process may gradually reduce material integrity.

Freeze–thaw weathering can be important in coastal regions where temperatures repeatedly cross the freezing point and sufficient water is present in pores and fractures.

Biological activity may also contribute to rock deterioration. Plant roots can enlarge existing fractures, while marine organisms may bore into or chemically modify exposed rock surfaces. Naylor *et al*. (2012) highlighted that biological activity can contribute actively to rocky-coast erosion and weathering. However, these effects are generally difficult to represent directly in slope-stability models and are more appropriately considered as part of the long-term environmental degradation of the rock mass.

Overall, chemical, thermal and biological processes may contribute to progressive weakening of coastal rock. However, their main engineering significance is that they can reduce material integrity and make the rock mass more sensitive to mechanical loading, rainfall and groundwater.

2.3.6 Summary

In summary, marine processes can affect coastal cliffs through both geometric change and material degradation. Wave action and abrasion may remove material and reduce toe support, while wetting–drying cycles, salt crystallization and other weathering processes can reduce the strength and stiffness of the remaining rock mass. Discontinuity properties and hydraulic behavior may also change as degradation develops. Importantly, the magnitude of these effects depends on lithology, rock structure and environmental conditions. Therefore, marine degradation should be represented using physically reasonable changes in engineering properties rather than by applying one universal reduction factor.

3. The case study

3.1 Introduction

This chapter describes the site conditions of the Mimi coastal cliff in North Taranaki, New Zealand, chosen representative case study in this thesis. The geological, geometric, structural and hydrogeological characteristics of the site are reported and are used to define the model geometry, material properties, groundwater conditions and discontinuity characteristics adopted in the subsequent analysis of the cliff stability.

The investigated cliff consists mainly of two geological units: the Rapanui Formation in the upper part of the cliff and the Mount Messenger Formation at the base. According to the available site information, these two units have different mechanical characteristics and are expected to respond differently to environmental loading. The Rapanui Formation is relatively weak and is more sensitive to weathering, rainfall infiltration and groundwater conditions. In comparison, the Mount Messenger Formation forms a stronger rock mass, and its behavior is more strongly influenced by discontinuities, weathering and marine erosion.

These differences are important for the numerical modelling because a single failure mechanism may not adequately represent the behavior of the whole cliff. Therefore, this chapter first describes the site location and cliff geometry, followed by the geological and structural conditions. The hydrogeological and rainfall conditions are then introduced, and the engineering parameters used in the numerical models are summarized. Finally, the expected failure mechanisms and the main uncertainties in the available data are discussed.

3.2 Site Location

The study site is located at Mimi on the North Taranaki coast of New Zealand (see figure 4). The Mimi cliff is directly exposed to coastal processes. Wave action affects the lower part of the cliff, while rainfall, groundwater movement and weathering act mainly from the landward and upper parts of the slope. The combined effect of these processes is important because degradation of the cliff toe may reduce the support of the upper slope, while rainfall and groundwater can weaken the relatively weak upper material.



Figure 4: Location of the Mimi study site on the North Taranaki coast, New Zealand (coordinate: -38.954948,174.444283; NZTM2000)

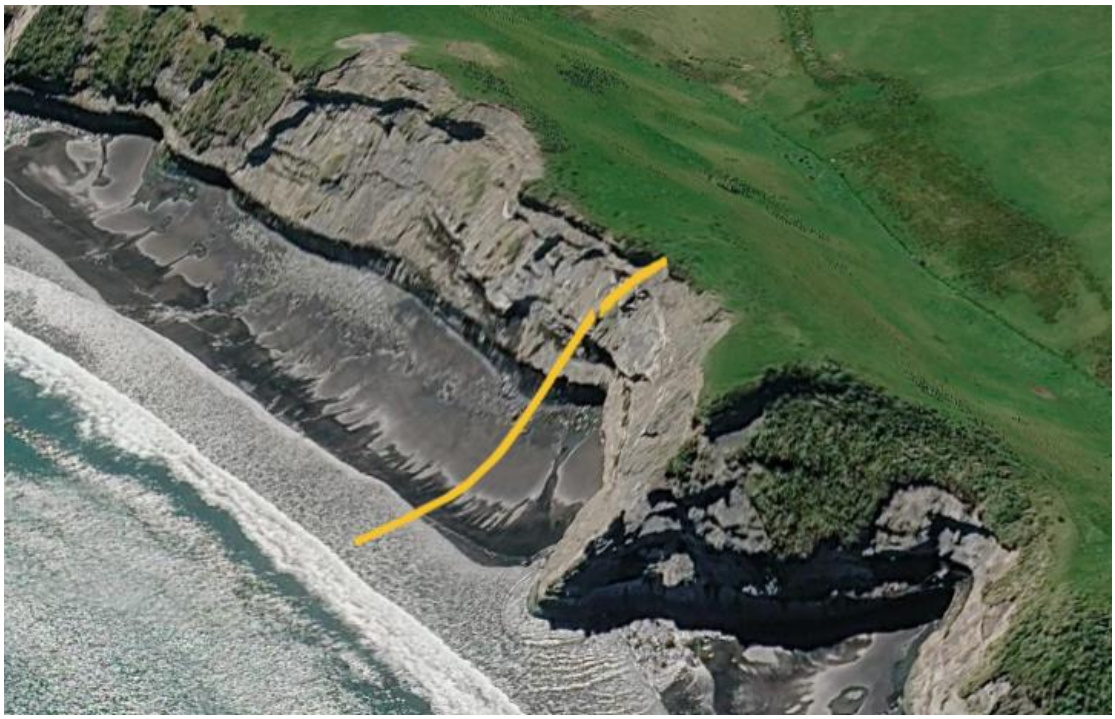


Figure 5：Aerial view of the Mimi coastal cliff (source: Google Earth)

3.3 Topography and Cliff Geometry

Cliff geometry directly affects stress distribution and slope stability and is therefore an important part of the modelling of the slope stability. For the Mimi site, pre- and post-change profiles are available from surveys carried out on 15 April 2023 and 14 December 2023, allowing changes in the cliff profile to be compared over this period (see figure 6).

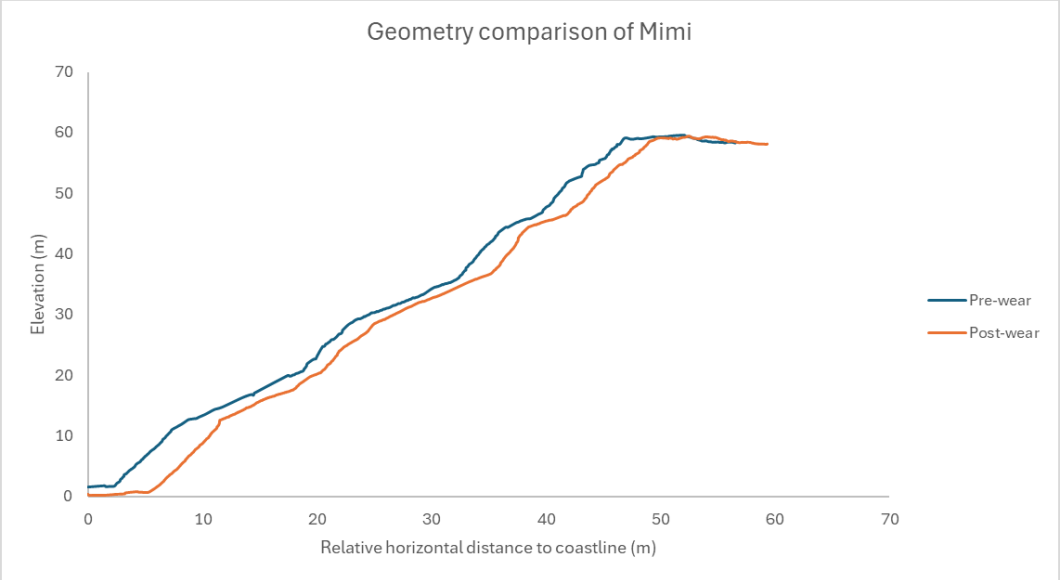


Figure 6: Comparison of the cliff profiles surveyed on 15 April 2023 and 14 December 2023

3.4 Geological Setting and Stratigraphy

As mentioned above, Mimi cliff is constituted by two main geological units: the Rapanui Formation in the upper part of the cliff and the Mount Messenger Formation in the lower part. A simplified stratigraphic profile, used for the stability analysis, is shown in figure 7.

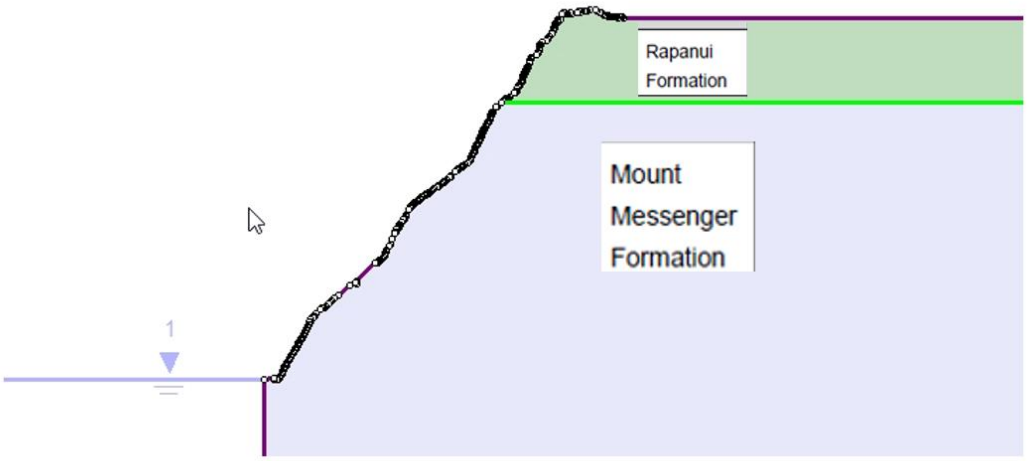


Figure 7: Simplified stratigraphic profile of the Mimi cliff

The available information characterizes the Rapanui Formation as predominantly massive to bedded silty mudstone with some interbedded sandstone layers. It is also described as being susceptible to weathering, particularly where rainfall infiltration and groundwater seepage weaken the material. From an engineering point of view, the Rapanui Formation is therefore treated as the weaker unit of the cliff.

The rock-mass structure of the Mount Messenger Formation has been described as generally massive to blocky, and its discontinuity surface conditions are mainly very good to good, although fair conditions can also occur. The rock mass can become very blocky and disturbed near fault zones.

The structure of the Mount Messenger Formation is important because discontinuities may control the deformation of the lower cliff even when the intact rock remains relatively strong. Observations from Mimi indicate the presence of steep to near-vertical joints. Some joints are approximately parallel to the cliff face and have been interpreted as possible stress-relaxation features (see figure 8).

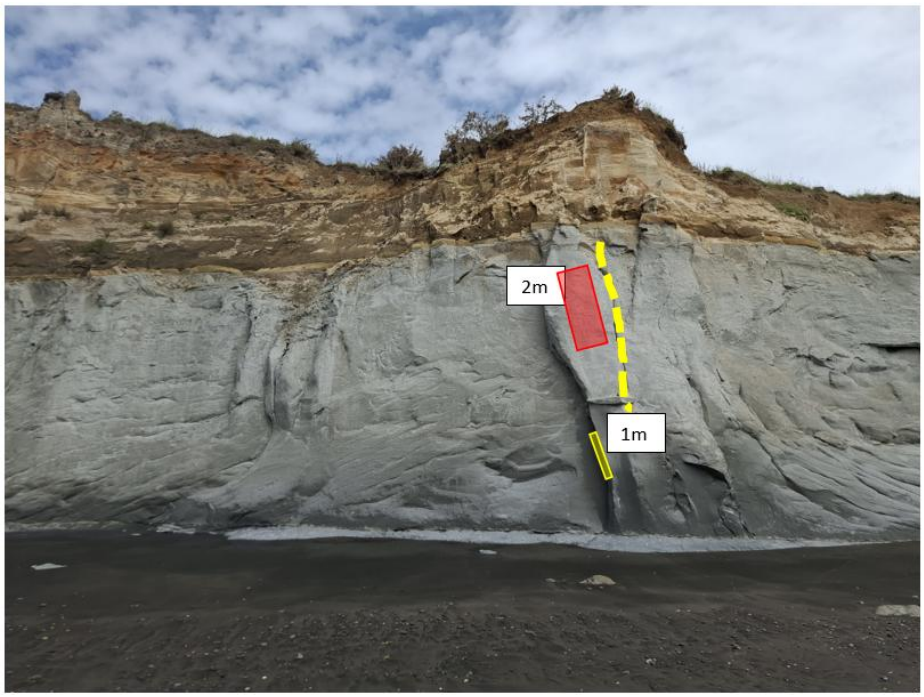


Figure 8: Representative discontinuities observed in the Mount Messenger Formation at Mimi.

The available structural dataset is relatively limited and contains only few measured pairs of discontinuity orientations. For this reason, the rock-mass structure was simplified into two representative joint sets (figure 9). Based on an assumed cliff-face orientation of approximately 50°/270°, the adopted joint geometry is summarized in Table 3.2.

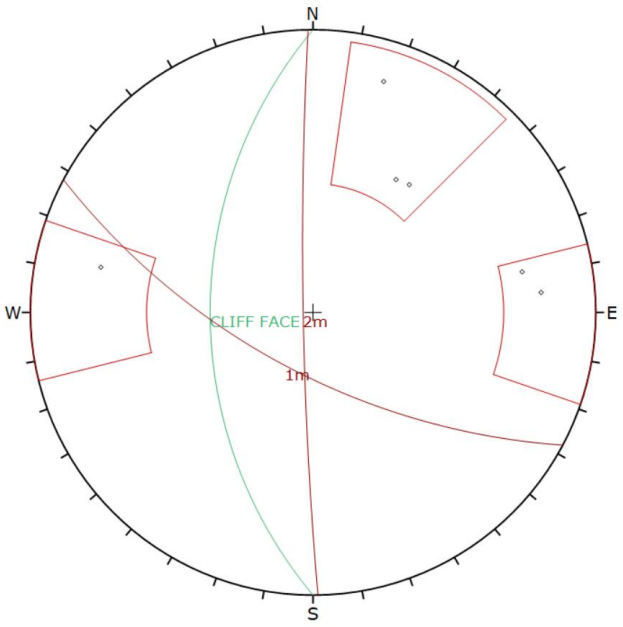


Figure 9: Orientation of the main discontinuity sets characterizing the Mimi cliff face

Table 1: discontinuity sets for the Mount Messenger Formation

Set	Orientation (DIP, DIP DIRECTION)	Spacing (mm)	Persistence (m)	Roughness
1m	(66°,208°)	233	≥1.5	Smooth or slightly rough
2m	(86°,269°)	167	About 1	Smooth or slightly rough
Cliff face	(50°, 270°)			

3.5 Hydrogeological and rainfall conditions

Groundwater is expected to affect the stability of the Mimi cliff, particularly within the upper Rapanui Formation. Site information indicates that seepage is often observed close to the approximate geological contact at around the 45 m level. This suggests that the contrast between the geological units may affect groundwater movement and drainage through the cliff.

Rainfall is included in the present study because it is expected to influence the hydraulic condition and stability of the Rapanui Formation. Rainfall infiltration can change pore-water pressures within the cliff and may reduce the effective resistance of weak and weathered material.

The rainfall data within available observation period (from 15th April 2023 to 14th December 2023) is obtained from website: Earth Science, New Zealand. The weekly rainfall data of the year of 2023 are summarized in figure 10.

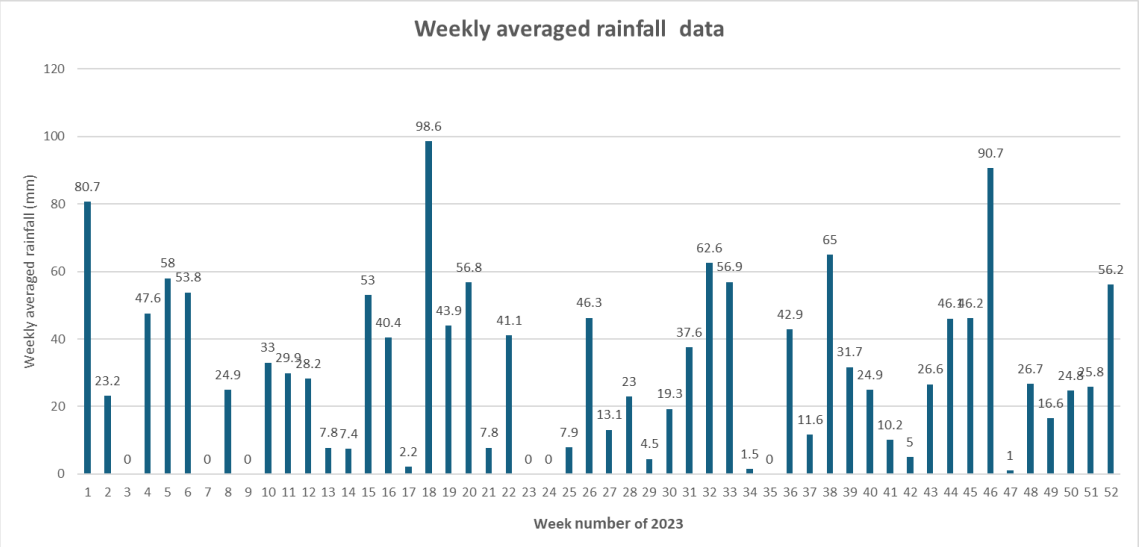


Figure 10: Weekly rainfall data of interested region

3.6 Mechanical Properties

Given the limited available data, the mechanical parameters of the rock masses adopted in previous modelling were derived from a combination of laboratory testing on intact rock, and values reported in previous studies, including Read *et al*. (2012) and Sivakugan *et al.* (2014). Therefore, these parameters should not all be regarded as directly measured, site-specific values

3.6.1 Mount Messenger Formation

For the Mount Messenger Formation, the intact-rock is characterized by a unit weight of 25 kN/m³, an intact uniaxial compressive strength of 35 MPa, an intact Hoek–Brown constant (m_i) of 5, an intact Young's modulus of 700 MPa and a Poisson's ratio of 0.30.

The intact UCS of 35 MPa and Young's modulus of 700 MPa were selected by considering both the available laboratory data in Table 2 and the observed condition of the Mount Messenger formation in the field (figure 8 above).

Table 2: Summary of Mount Messenger formation

Lithology[a]	Unconfined compression					Indirect tensile strength σ_t (MPa)		
	Tests	Strength q_u (MPa)		Tangent modulus E_t (MPa)				
		Range	Average	Range	Average	Tests	Range	Average
Sandstone	12	0.1 – 2.7	1.5	4 – 390	230	10	0.04 – 0.06	0.04
Sandy / Silty – stone	7	0.6 – 5.3	2.8	60 – 670	235	7	0.14 – 0.69	0.33
Siltstone	8	0.8 – 7.0	4.5	30 – 615	290	8	0.17 – 0.60	0.29
slightly calcareous	5	8.2 – 20.4	12.9	730 – 5,500	2,230	5	0.08 – 0.37	0.17
Concretion	10	35 – 157	106	30,000 – 105,000	66,000	12	0.6 – 12.6	8.4
Harder layers [1]	1		12.0		4,850	3	3.4 – 5.4	4.6

Note: [1] Single compressive result in harder layers is a sandstone that is fossiliferous rather than calcareously cemented.

Source: laboratory data provided by Saskia and Dickson (2026), University of Auckland

From figure 8, the Mount Messenger (grey stone) appears relatively massive and well cemented, suggesting mechanical properties towards the stronger end of the tested lithologies. Accordingly, a UCS of 35 MPa was adopted as a conservative value representative of relatively strongly cemented intact material, while a Young's modulus of 700 MPa was selected close to the upper range reported for sandy/silty-stone (670 MPa) and the lower range of more strongly cemented material (approximately 730 MPa).

A GSI value of 60 was adopted based on the GSI index (figure 11), together with field observations of the exposed Mount Messenger sandstone. The rock mass is generally blocky, with relatively large intact blocks separated by limited set of joints. These characteristics correspond approximately to a blocky rock mass with good-to-fair

surface conditions on the GSI chart, giving a representative GSI value of about 60.

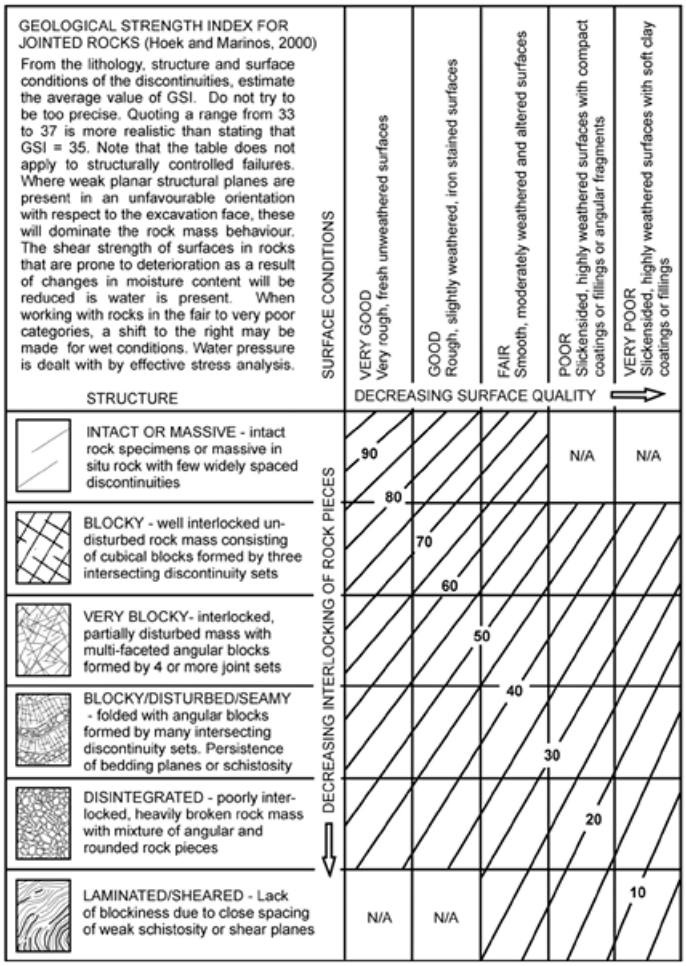


Figure 11: GSI index by Hook & Brown (2000)

Weathering was assumed to be higher in the lower part of the face in Mount Messenger formation and a bit lower in the upper part. For this reason, 2 different level of weathering have been considered, represented by reducing the GSI and the corresponding rock-mass strength and stiffness. A GSI of 50 was reasonably adopted for weakly weathered material and a GSI of 40 for highly weathered material. For each GSI value, the corresponding rock-mass strength and deformation parameters were recalculated using the Hoek–Brown criterion, thereby representing the progressive reduction in rock-mass quality with increasing weathering. The main strength parameters are summarized in table 3.

The reduction in GSI from 60 to 40 represents progressive deterioration of rock-mass quality. All the mechanical parameters of the rock mass are reduced accordingly. This procedure is reasonable when experimental data are not available.

Table 3: Main properties of Mount Messenger Formation

	Intact rock	Normal Rock mass	Weakly weathered Rock mass	Highly weathered Rock mass	Unit
Unit weight (γ)	25	25	25	25	kN/m^3
Intact UCS (σ_{ci})	35	35	35	35	MPa
m_i	5	5	5	5	-
Young's modulus (E)	700	364	215	112	MPa
Poisson's ratio	0.3	0.3	0.3	0.3	-
GSI	-	60	50	40	-
Cohesion (c)	-	0.78	0.5	0.375	MPa
Friction angle (φ)	-	42^o	40^o	37^o	°

3.6.2 Rapanui Formation

The mechanical properties of Rapanui Formation were collected in table 4. The material mechanical parameters for the normal (unweathered) condition were defined through numerical back-analysis in RS2, using the site information and material data provided by the research team as the initial basis. The model was progressively calibrated to reproduce a condition close to failure while remaining stable. During this calibration, cohesion were the primary parameters adjusted, whereas the other material properties were kept unchanged.

Table 4: The main material strength parameters of Rapanui formation

Parameter	Normal	Weathered	Unit
Unit weight (γ)	19	-	kN/m^3
Cohesion (c)	0.015	0.010	MPa
Friction angle (φ)	35	30	°
Compressive strength	0.058	0.034	MPa
Tensile strength	0.006	0.0034	MPa
Young's modulus (E)	180	180	MPa
Poisson's ration (ν)	0.3	0.3	-

These values show a clear mechanical contrast between the two geological units. The Rapanui Formation has relatively low strength and is therefore more likely to control the overall continuum stability of the cliff. The Mount Messenger Formation is stronger, but the presence of joints means that local failure can still develop through structural mechanisms.

3.6.3 Joint Properties

Due to the lack of data about joint properties, the discontinuities, a preliminary joint friction angle of 30° was reasonably assumed. The joint persistence was examined by the observation of their length on the cliff face, of about 70%, while normal and shear stiffness were assumed as suggested in the numerical code used for numerical stability analysis.

3.7 Data Quality and Uncertainty

Several uncertainties remain in the site data used to construct the models for the stability analysis. These uncertainties need to be recognized because they influence the interpretation of the calculated factor of safety, deformation and joint response.

The first uncertainty is related to the discontinuity data. Only six pairs of discontinuity orientations were available for defining the structural condition of the Mount Messenger Formation. The two joint sets used in the model therefore represent a simplified interpretation of the available measurements. In particular, joint persistence may vary considerably in the field and cannot be fully defined from the current dataset.

The second uncertainty is associated with groundwater conditions. Although seepage has been observed near the approximate geological contact, there is little direct information on the groundwater conditions within the Rapanui Formation. No continuous groundwater monitoring data are currently available. Therefore, the hydraulic boundary conditions used in the model should be regarded as an engineering interpretation rather than an exact representation of the field groundwater system.

The third uncertainty concerns the mechanical parameters. The adopted values were obtained from a combination of laboratory testing, previous reports, published literature and engineering interpretation. As a result, some parameters are better constrained than others. The intact-rock properties have a clearer basis, while weathered rock-mass properties, hydraulic parameters and joint properties contain a higher level of subjectivity.

These uncertainties have been considered when interpreting the results of the stability analyses. Where appropriate, different modelling scenarios and sensitivity analyses have been used to examine how changes in rainfall, weathering and structural conditions affect the predicted cliff response.

4. Methodology and numerical modelling

4.1 General workflow

In order to investigate the stability, the Taranaki coastal cliff, Mimi, under progressive

environmental conditions, a numerical approach has been used. In particular, the Finite Element Method was chosen for performing 2D analyses on a transversal representative section of the cliff. The joins sets were introduced in the model. RS2 code (Rocscience) was used for this purpose. The basic modelling strategy was designed not only to calculate the factor of safety of the cliff, but also to analyze separately the influence of rainfall infiltration, rock-mass degradation, and the long-term effects of wave action on the cliff stability.

The workflow started with the geological model based on the site information described in Chapter 3. The cliff geometry, lithological boundaries, weathered zones, groundwater conditions, and relevant material properties were first transferred into a two-dimensional numerical representation. A baseline model was then established to provide a reference condition against which the effects of subsequent changes could be assessed.

An initial groundwater condition was first generated before rainfall was introduced. Following the baseline model, the hydraulic condition of the cliff was established. A transient seepage analysis was adopted to represent the time-dependent hydraulic response of the cliff. The seawater acting on the submerged ground was represented by a ponded water load, producing a hydrostatic pressure that increases linearly with water depth. The detailed boundary condition will be discussed in later sections. Rainfall infiltration was then simulated, with rainfall represented at different temporal resolutions depending on the purpose of each scenario.

Rock-mass degradation was introduced in later stages of the modelling. Two degradation mechanisms were distinguished. The first represented weathering-related deterioration of the exposed cliff material, while the second represented the reduction in mechanical properties in the lower slope and toe region associated with long-term wave action. This distinction was made because rainfall-induced weathering and marine erosion do not necessarily affect the same part of the cliff or operate through the same physical mechanism.

4.2 Introduction of Numerical Software and Analysis Type

The numerical analyses were conducted using RS2, a two-dimensional finite-element program developed for geotechnical and rock engineering applications. RS2 was selected because it allows mechanical deformation, groundwater flow, pore-water pressure development, material heterogeneity, and shear strength reduction to be analyzed within a common modelling environment.

A two-dimensional plane-strain condition was assumed throughout the analysis. Under

this assumption, deformation perpendicular to the modelled cross-section is considered negligible. This simplification is appropriate where the selected cliff section can reasonably be treated as laterally continuous over a sufficient distance relative to the dimensions of the expected failure mechanism. The limitation of this assumption is recognized because natural coastal cliffs may exhibit three-dimensional variability along the coastline. However, the purpose of the present study was to examine the relative effects of hydro-mechanical and degradation processes on a representative cliff cross-section rather than to reproduce the complete three-dimensional coastal morphology.

The numerical modelling procedure involved 3 main types of analysis related to water: a static water condition, steady-state groundwater analysis, transient groundwater analysis. According to RS2 manual, the static water condition provided a simplified hydrostatic pore-water pressure distribution based on a prescribed groundwater level. Steady-state analysis was used to establish an equilibrium seepage condition in which the hydraulic field remained constant with time. Transient groundwater analysis was subsequently used to simulate the time-dependent response of the cliff to rainfall infiltration, including changes in pore-water pressure, hydraulic head and saturation.

Slope stability was evaluated using the shear strength reduction (SSR) method implemented in RS2. This approach progressively reduces the available shear strength of the materials until the numerical model can no longer maintain a stable equilibrium state. The resulting strength reduction factor is interpreted as the global factor of safety.

The numerical programme was organised into four principal scenarios with progressively increasing levels of environmental complexity. Scenario 1 represented the baseline cliff condition and adopted a static water condition without rainfall or material degradation. Scenario 2 introduced rainfall infiltration using the selected groundwater-flow analysis while maintaining the original material properties. Scenario 3 further incorporated weathering-related degradation together with a more detailed rainfall representation. Scenario 4 considered additional mechanical degradation in the lower slope and toe region associated with long-term wave action. Shear strength reduction analysis was performed for Scenarios 1–3, whereas Scenario 4 was assessed using the corresponding mechanical and hydraulic response without an additional SSR calculation.

An important distinction in this study is that the effect of wave action was not necessarily simulated as a short-term dynamic wave load. Instead, where direct cyclic wave loading was not explicitly modelled, the long-term influence of marine action was represented through degradation of the mechanical properties of the lower slope and

toe materials. This approach is consistent with the principal objective of the study, which is to investigate progressive cliff weakening rather than the response to an individual wave impact.

4.3 Model Geometry and Domain Size

The numerical model geometry was developed from the representative cliff cross-section established in Chapter 3. The selected section was chosen because it captured the principal morphological and geological characteristics relevant to the stability analysis, including the cliff crest, main slope face, lower slope, toe region, geological boundaries, and the distribution of weathered material. In addition, in order to increase the calculation efficiency, the geometry of the slope has been automatically simplified within RS2 by reduce the vertices to 20% of original data.

The modelled cliff had an approximate height of 65 m. The external numerical boundaries were positioned sufficiently far from the cliff to minimise their influence on the calculated deformation and failure mechanism. The lateral boundary behind the cliff crest was located beyond the expected deformation zone, while the lower boundary was placed sufficiently deep to avoid artificially controlling the shape of the failure mechanism. Therefore, the horizontal extent of the numerical domain was 365 m, while the model base extended to approximately 110 m below the principal zone of interest.

To increase the analysis accuracy, and avoid numerical instabilities, the profile of the section was obtained by the excavation of 15 layers. The numerical model for the cliff is presented in figure 12.

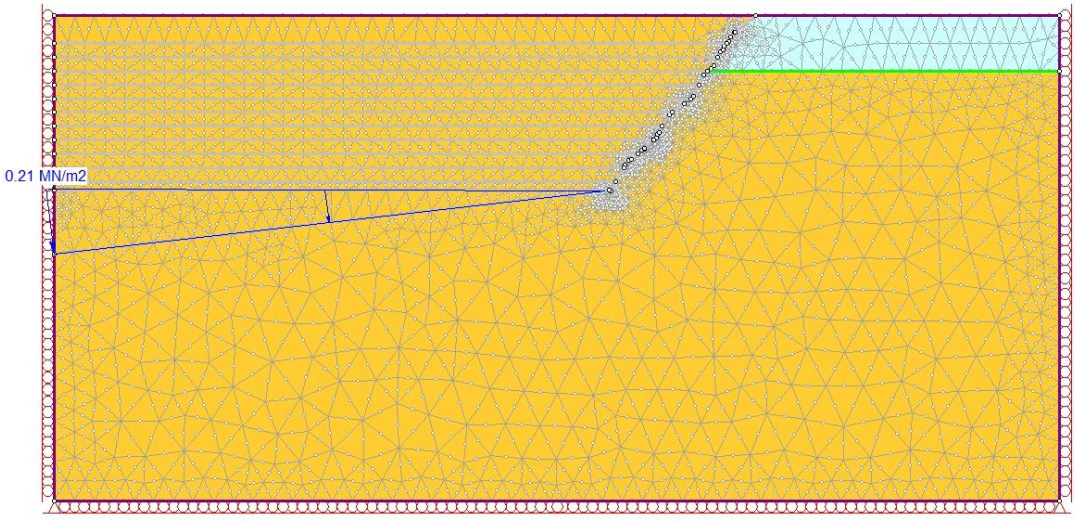


Figure 12: Geometry of numerical cliff model (before excavation)

4.4 Mesh setup

The numerical domain was discretized using 6 nodded triangular finite elements.

A graded mesh was adopted so that greater numerical resolution could be provided in regions where higher stress, strain or hydraulic gradients were expected, while avoiding an unnecessarily fine mesh throughout the entire domain. Local refinement was applied in particular around: the cliff face, geological or material boundaries; areas where localized deformation was anticipated. The representation of the mesh setup is also indicated in figure 12.

4.5 Mechanical Properties of the Materials

The materials were represented as continuum/equivalent materials, and the Mohr–Coulomb strength parameters were adopted.

The detailed data will be given in the later sections.

4.6 Scenario 1: Baseline condition

4.6.1 Introduction

Scenario 1 was established as the reference condition for the entire numerical modelling programme. The purpose of this scenario was to evaluate the basic stability of the cliff before rainfall infiltration, weathering-related deterioration, or additional degradation caused by marine processes was introduced. It therefore provides the reference against which the subsequent scenarios are compared.

The baseline model adopted the cliff geometry and geological stratigraphy established from the site characterization presented in Chapter 3. No additional weathered or wave-degraded zones were introduced at this stage, and the original mechanical properties assigned to each geological unit were retained.

The rock masses (Mount Messenger and Rapanui) were represented without inserting individual discontinuities. The principal analysis was therefore based on an equivalent continuum representation.

4.6.2 Water condition

A static water condition was adopted for the baseline model. The use of static water was considered appropriate because Scenario 1 was intended to provide a controlled reference condition (natural static condition) rather than reproduce the complete natural groundwater-flow system

A prescribed groundwater table was defined based on the sea level, from which the corresponding hydrostatic pressure distribution was calculated. Just as it is shown in figure 12.

In addition, it is assumed that the cliff slope does not contain any water in such condition, which seem to be the usual condition of the cliff.

4.6.3 Mechanical parameters

As it is stated before, the model contains 15 excavation stages. At the first stage, both Rapanui formation and Mount Messenger formation is considered behaving elastically. The material was assumed to be elastic during the initial stage to establish the in-situ stress field without generating artificial plastic strains. The elasto-perfectly plastic constitutive model was subsequently activated for both the formations during the excavation stages so that yielding could be attributed primarily to excavation-induced stress re-distribution.

The assigned key parameters are presented in table 5 below:

Table 5: Material properties for scenario 1

Material	Unit weight kN/m^3	Young's modulus (MPa)	Poisson's ratio	Tensile strength (MPa)	Friction angle	Cohesion (MPa)
Rapanui formation (elastic)	19	180	0.3	0.006	35	0.015
Mount Messenger formation (elastic)	25	364	0.3	0.343	42^o	0.78
Rapanui formation (perfectly plastic)	19	180	0.3	0.006	35^o	0.015
Mount Messenger formation (perfectly plastic)	25	364	0.3	0.343	40^o	0.5

4.7 Scenario 2: Rainfall action without Weathering

4.7.1 Introduction

Scenario 2 was developed to investigate the effect of rainfall-related groundwater conditions while maintaining the same mechanical properties as the baseline model. It is expected to investigate if the rainfall is the main triggering factor for the instability

and cliff retreat. Therefore, the principal difference between Scenarios 1 and 2 was hydraulic rather than mechanical.

The cliff geometry, geological boundaries, mesh configuration and mechanical boundary conditions used in Scenario 1 were retained. Similarly, the original mechanical properties of the geological materials were maintained. No weathering-related strength reduction was introduced, and no additional wave-induced degradation was applied to the lower slope.

4.7.2 Rainfall representation

Rainfall in Scenario 2 was represented using heaviest weekly averaged rainfall data. During the rainfall record interval, the measured rainfall record was averaged over weekly intervals and the heaviest rainfall weekly interval was introduced into the groundwater model.

The weekly averaged rainfall data was reported in figure 10 previously. It can be obtained that the heaviest rainfall amount is 98.6 mm. When introducing into RS2, this value should be converted as rainfall infiltration rate, which is equivalent to 1.9×10^{-7} m/s in a weekly interval. This rainfall infiltration has been activated on the all-cliffs boundary which exposed to air. The adopted rainfall duration is 1 week, while only 6 days have rainfall records, corresponding to 518400 seconds.

4.7.3 Grounder water settings and material hydraulic properties

Unlike the static water representation used in Scenario 1, Scenario 2 incorporated a groundwater-flow analysis so that the influence of rainfall on pore-water pressure could be represented. To achieve this, transient analysis method was adopted rather than static water method.

To active transient analysis, the hydraulic properties and groundwater boundary conditions should be defined.

The hydraulic properties of materials should be chose based on the real behavior of the cliff. As it is already discussed in Chapter 3, a phenomenon of seepage was observed at the contact boundary of two formations. Also, the material of the lower part of the cliff, Mount Messenger formation, is good rock mass. Therefore, its hydraulic conductivity can be reasonably assumed far lower than it in Rapanui formation. However, due to the lack of data, the selection of the hydraulic conductivity of the Rapanui formation is obtained from literatures research in the close area, and a hydraulic conductivity near 0 is selected for Mount Messenger formation.

The hydraulic conductivities for 2 formations are reported in table 6.

Table 6: hydraulic conductivities for 2 formations in scenario 2

Material	Hydraulic conductivity m/s
Rapanui formation (elastic)	1×10^{-7}
Mount Messenger formation (elastic)	1×10^{-10}
Rapanui formation (perfectly plastic)	1×10^{-7}
Mount Messenger formation (perfectly plastic)	1×10^{-10}

The mechanical boundary condition is remained as the same as Scenario 1, and the hydraulic boundary is shown in figure 13.

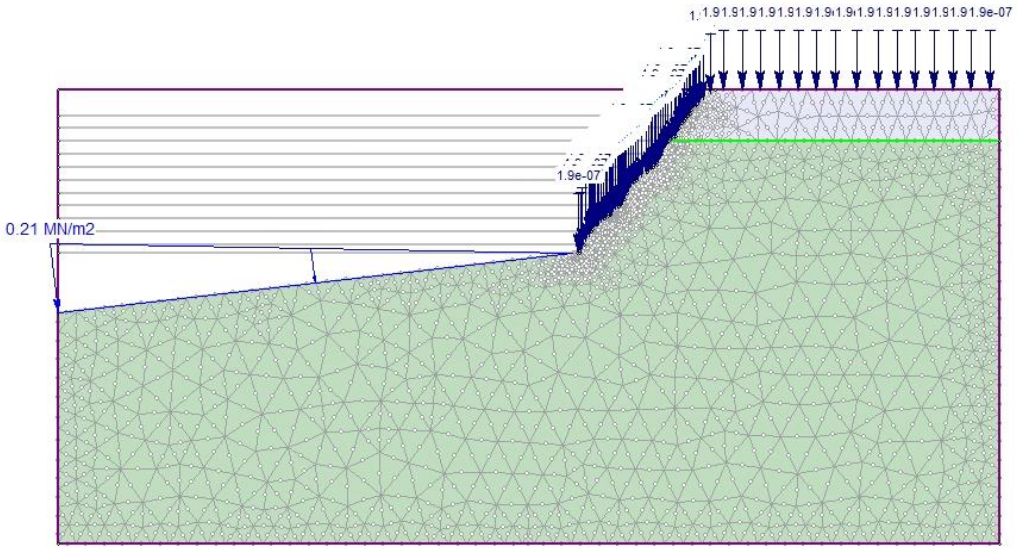


Figure 13: Numerical model for scenario 2 (including water boundary condition)

4.8 Scenario 3: Rainfall Condition with Weathering

4.8.1 Introduction

Scenario 3 was developed to investigate the combined effects of rainfall infiltration and weathering-related deterioration on the stability of the cliff. In contrast to the previous scenarios, weathering was introduced as a spatially variable material condition rather than through a uniform reduction in rock-mass properties.

In this scenario, the continuum model and the equivalent-continuum model were adopted for Rapanui formation and Mount Messenger formation, respectively. Two rainfall inputs were applied separately: weekly averaged rainfall and daily averaged rainfall. The same geometry, weathering distribution, hydraulic parameters and boundary conditions were maintained between the corresponding rainfall cases. This arrangement allowed both the influence of rock-mass representation and the sensitivity

of the weathered cliff to rainfall temporal resolution to be examined.

In general, the numerical models are almost remained the same as previous scenarios other than weathered material properties and rainfall infiltration rate.

4.8.2 The Effect of Weathering on Material properties

Weathering in Scenario 3 was introduced according to its expected spatial development from the exposed cliff boundaries.

Based on the cliff-retreat characteristics identified in Chapter 3, material located within approximately 3 m of the exposed model boundary was considered to have been affected by weathering. The weathering zone was measured inward from the exposed cliff surface so that its geometry followed the actual slope profile rather than being represented as a simple vertical or horizontal layer.

Within this 3 m zone, the original material properties were replaced by the corresponding weathered mechanical properties determined in Chapter 3. Material located outside this zone retained its original properties.

A higher degree of degradation was assigned to part of the Mount Messenger Formation in the lower section of the cliff. This was because the lower cliff is subjected not only to conventional subaerial weathering but also to repeated marine influence. The elevation affected by marine processes was estimated by considering the observed wave environment together with variations in water level associated with tides and seasonal changes in sea level. In addition to normal atmospheric weathering, this zone may be influenced by repeated wave impact, wetting and drying cycles, tidal fluctuations, seasonal changes in water level, abrasion and prolonged exposure to marine conditions.

On this basis, a boundary was defined at approximately 15 m above the adopted sea-level datum within the Mount Messenger Formation.

Material above this elevation, where it fell within the defined surface weathering zone, was assigned the weakly weathered condition. Material below the approximately 15 m elevation boundary and within the affected lower-cliff region was assigned a highly weathered condition.

Importantly, the model does not attempt to simulate individual wave impacts dynamically. The marine influence is represented through the resulting long-term deterioration of the lower-cliff material.

The layout of material at different weathered level is shown in figure 14, and the mechanical properties of each material are reported in table 7.

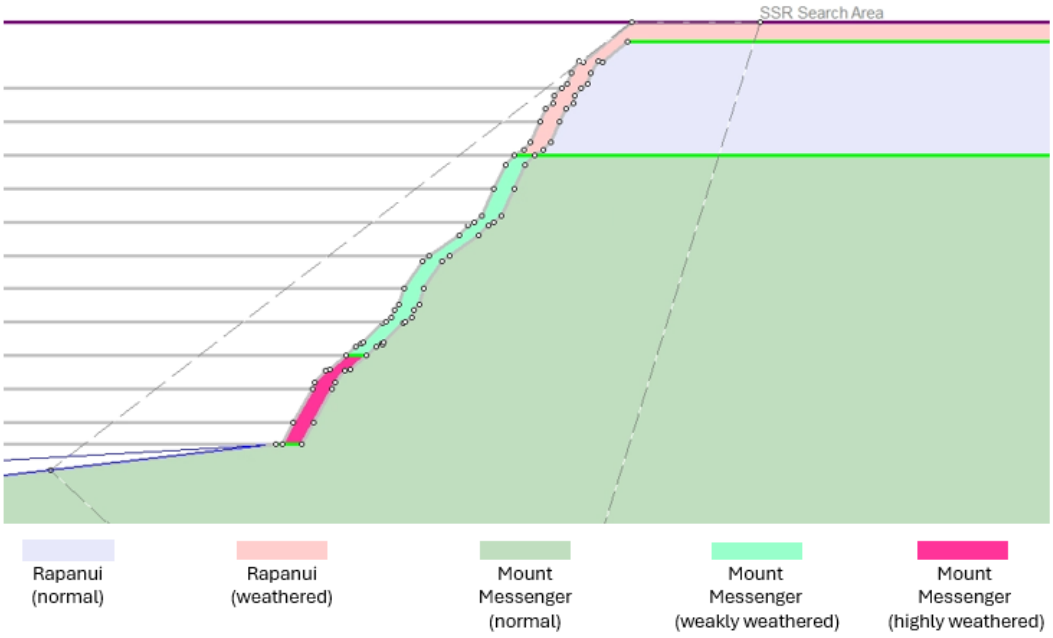


Figure 14: The geological layout of materials for scenario 3

Table 7: Main mechanical properties of materials involved in scenario 3

Material	Unit weight kN/m^3	Young's modulus (MPa)	Poisson's ratio	Tensile strength (MPa)	Friction angle	Cohesion (MPa)
Rapanui (normal)	19	180	0.3	0.006	35	0.015
Rapanui (weathered)	19	180	0.3	0.0034	30 °	0.01
Mount Messenger (normal)	25	364	0.3	0.343	42°	0.78
Mount Messenger (weakly weathered)	25	215	0.3	0.161	40°	0.5
Mount Messenger (highly weathered)	25	112	0.3	0.076	37°	0.375

4.8.3 Weekly averaged and Daily Rainfall

Two rainfall representations were applied independently to the same weathered cliff configurations.

The first used weekly averaged rainfall, while the second used daily rainfall in the same week.

Both rainfall records were derived from the same underlying rainfall dataset and

covered the corresponding analysis period. The use of both rainfall resolutions served an additional methodological purpose. Once the material had already been weakened by weathering, its stability could potentially become more sensitive to changes in groundwater condition. Weekly averaging may suppress short-duration rainfall peaks, whereas daily rainfall retains these variations and may therefore generate a different transient pore-pressure response.

4.9 Scenario 4: with joints

4.9.1 Introduction

Scenario 4 was the most structurally detailed model in the numerical programme. While Scenario 3 represented the influence of rock-mass structure through continuum and equivalent-continuum material properties, Scenario 4 adopted a different treatment for the Mount Messenger Formation. In this scenario, the formation was represented using the mechanical properties of the intact material together with explicitly defined discontinuities.

The purpose of this change was to examine whether the response of the lower cliff was controlled not only by the overall reduction in rock-mass strength, but also by the presence and mechanical behavior of individual discontinuities.

Unlike the equivalent-continuum approach, which distributes the influence of discontinuities throughout a homogenized rock mass, the jointed model allows normal/shear displacements along the discontinuity interfaces.

The overall cliff geometry, major geological boundaries and numerical domain were maintained consistently with the preceding scenarios. The weathering framework established in Scenario 3 was also retained. Material located within approximately 3 m of the exposed cliff boundary was considered weathered according to the retreat-based interpretation described in Chapter 3.

Just as Scenario 3, in the lower Mount Messenger Formation, the approximately 15 m elevation boundary was retained to distinguish between the weakly weathered and more strongly marine-affected portions of the cliff.

The principal difference in Scenario 4 was the way in which the mechanical behavior of the Mount Messenger Formation was represented. The mechanical properties of Rapanui formation and the weakly/highly weathered Mount Messenger formation are remained unchanged.

4.9.2 Representation of the Mount Messenger Formation

In an equivalent-continuum model, the influence of fractures and discontinuities is incorporated indirectly by reducing the mechanical properties of the bulk material. Although this approach is appropriate for investigating the overall behavior of a fractured rock mass, it does not reproduce the mechanical response of a rock mass when this is conditioned by the presence of discontinuities (discontinuum medium). In this scenario, the representation of original Mount Messenger formation is therefore done by intact rock with joints.

4.9.3 Discontinuity Geometry and Mechanical Properties

The discontinuities within the Mount Messenger Formation, belong to the 2 sets defined in Chapter3, and the mechanical properties for intact Mount Messenger formation were defined according to the structural information established in Chapter 3.

The numerical model of Scenario 4 is shown in Figure 15, which clearly indicates the geometry of the joint layout. It should be noted that explicit discontinuities were introduced only within a selected portion of the Mount Messenger Formation rather than throughout the entire formation. The extent of the jointed region was checked by increasing the size of the area containing explicit discontinuities, and no significant change in the analysis results was observed. This confirmed that the selected jointed area was sufficiently large to capture the relevant failure mechanism. Extending the discontinuity network throughout the complete formation would have substantially increased the number of discrete elements and the overall computational demand of the model, while providing limited additional information for the specific mechanism investigated in this scenario.

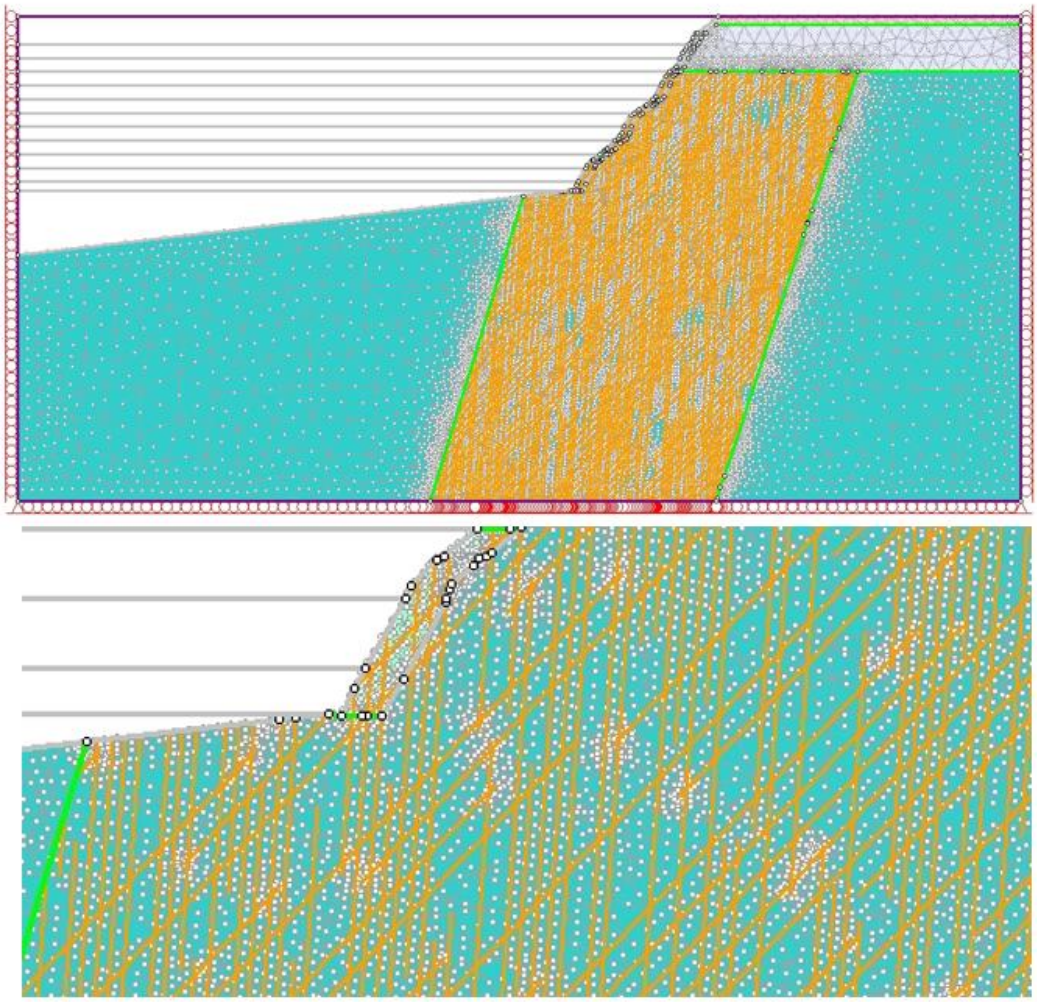


Figure 15: Numerical model for scenario 4 (top: global model; bottom: zoomed jointed area)

5. Results

5.1 Introduction

This chapter presents the results obtained from the numerical analyses described in Chapter 4. The results are organised according to the four modelling scenarios, which were developed progressively to examine the effects of rainfall infiltration, weathering, wave-related material degradation, and rock mass discontinuities on the stability and retreat behaviour of the investigated coastal cliff.

This Chapter will show the calculated factor of safety, pore-water pressure distribution, displacement pattern, shear strain concentration, and the development of localised instability. The implications of these results and their relationship with the observed

cliff retreat are discussed further in Chapter 6.

As it is described in previous Chapter, for Scenarios 1–3, the overall stability of the slope was assessed using the SSR method in RS2. The critical strength reduction factor obtained at failure is reported as the factor of safety. Scenario 4 was treated differently. Because the upper part of the model was already highly unstable and the purpose of this scenario was to investigate the deformation and retreat behaviour of the lower cliff, a global factor of safety related to the whole model would not be representative. For this reason, SSR was not undertaken. Instead, the results were examined directly in terms of displacement, strain localisation and deformation associated with the explicitly represented discontinuities.

5.2 Scenario 1

5.2.1 Stability and Stress Distribution

The SSR analysis returned a critical SRF of 1.08. (see figure 16)

At the critical stage, Sigma 1 ranged from approximately 0 MPa to 4.22 MPa. The stress values generally increased with depth, with the highest values occurring close to the base of the model. The stress contours also showed noticeable changes in shape around the transition between the lower slope and the steeper cliff face.

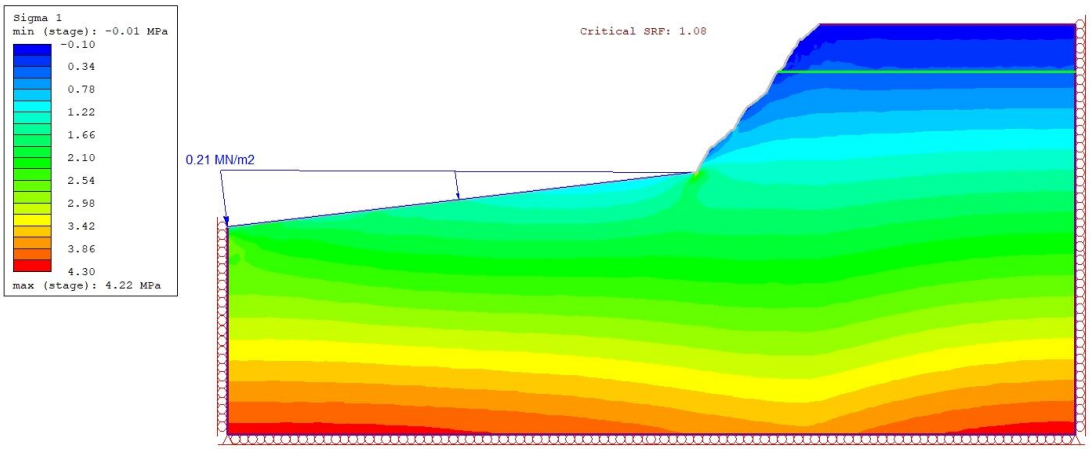


Figure 16: Major principal stress (Sigma 1) distribution at the critical SRF of 1.08 for Scenario 1.

5.2.2 Plastic Strain and Yielded Elements

The distribution of maximum shear plastic strain at the critical stage (i.e. under limit conditions of stability) is shown in Figure 17.

The maximum shear plastic strain reached approximately 0.774. The highest strain values were concentrated within the upper part of the cliff, in the Rapanui formation. A narrow zone of elevated plastic strain extended from the cliff face towards the upper

slope and crest. In comparison, most of the lower Mount Messenger formation remained at very low plastic strain levels.

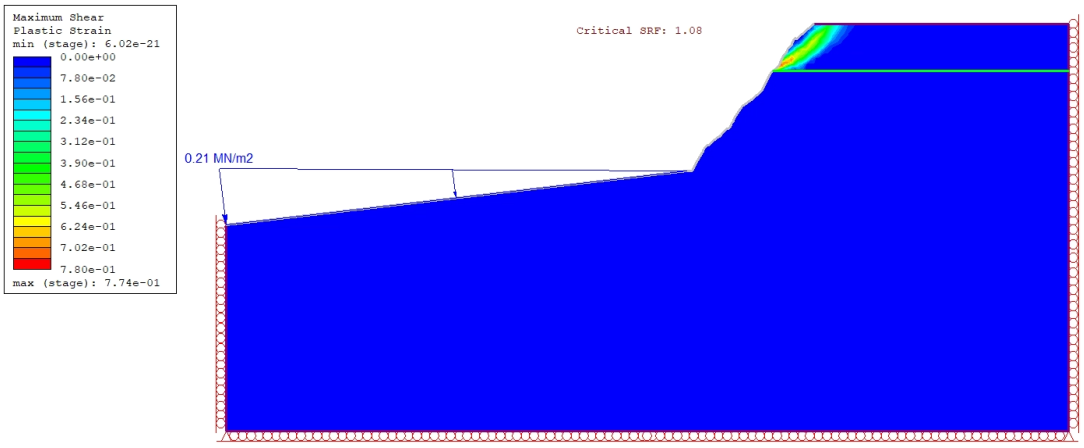


Figure 17: Maximum shear plastic strain distribution at the critical SRF of 1.08 for Scenario 1

The yielded-element results showed a similar spatial distribution (figure 18). A large proportion of the Rapanui material was yielded at the critical stage. The highest percentage of yielded elements occurred close to the upper slope surface. In the Mount Messenger formation, most of the rock mass remained unyielded. A small localised yielded zone was also observed near the lower slope break.

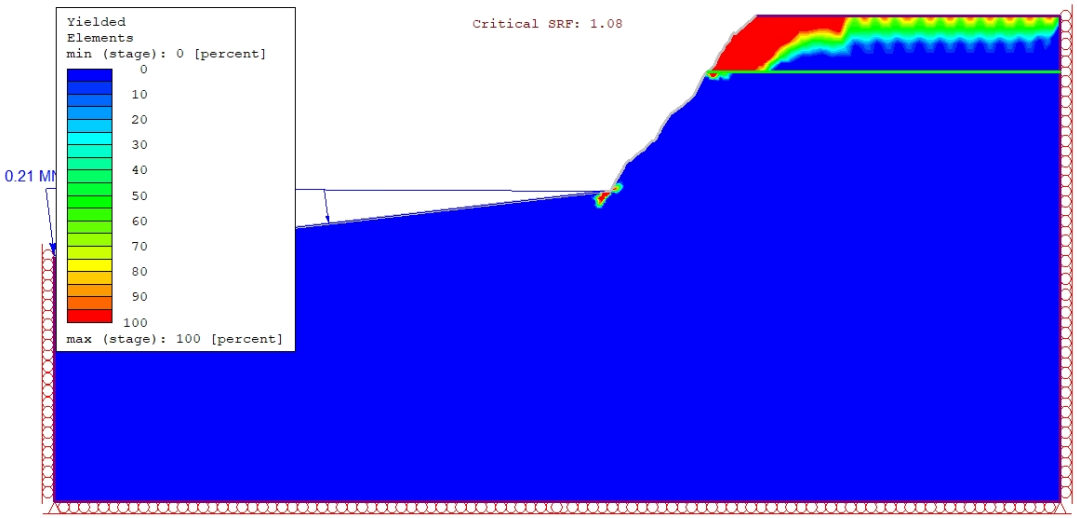


Figure 18: Distribution of yielded elements at the critical SRF of 1.08 for Scenario 1

5.3 Scenario 2

5.3.1Stability and Hydraulic Response

The SSR analysis returned a critical SRF of 0.62. The hydraulic condition at the critical stage is presented in figure 19.

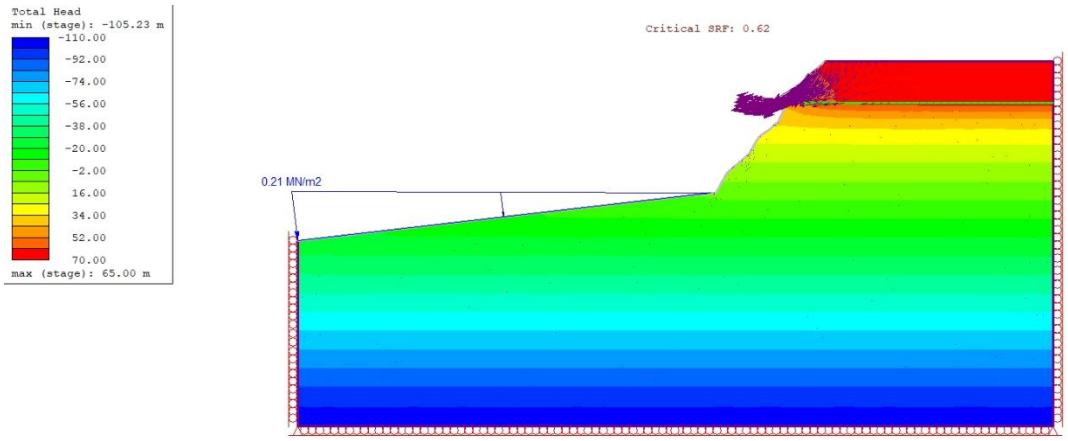


Figure 19: Total head distribution and groundwater flow directions at the critical SRF of 0.62 for Scenario 2

The groundwater flow vectors shown in figure 18 were concentrated mainly within the upper slope, at the boundary of the 2 formations. The arrows show the direction of groundwater flow, with flow occurring towards the exposed cliff face.

5.3.2 Yielded Elements

The distribution of yielded elements at the critical stage is shown in figure 20.

A large yielded zone was observed within the upper part of the cliff. Much of the near-surface material in this region reached a high percentage of yielded elements, with values approaching 100% over a substantial area.

The yielded zone extended from the upper cliff face towards the crest and continued laterally across part of the upper material. Below the Rapanui formation, most of the underlying rock mass remained unyielded

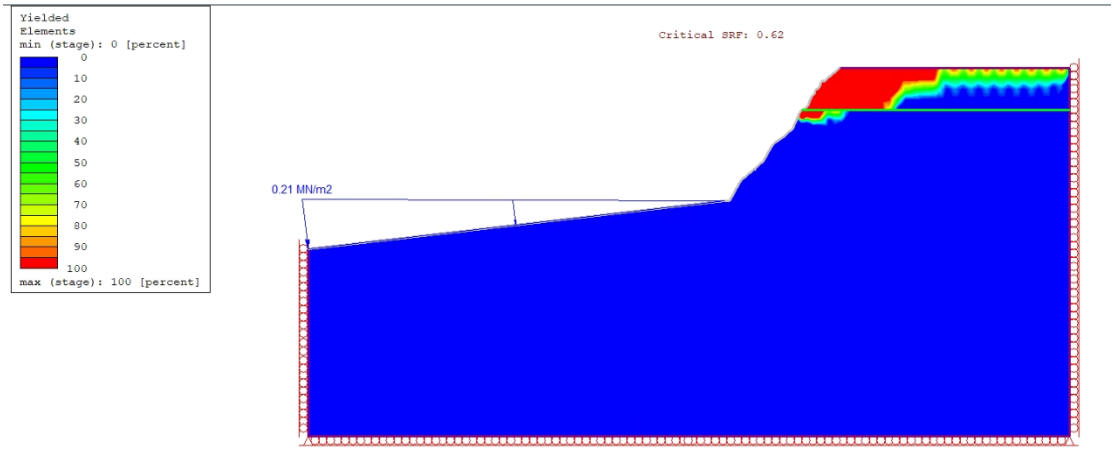


Figure 20: Distribution of yielded elements at the critical SRF of 0.62 for Scenario 2

5.3.3 Maximum Shear Plastic Strain

The maximum shear plastic strain distribution at the critical stage is presented in figure 21.

The maximum shear plastic strain reached approximately 33 at the critical stage. Elevated strain was concentrated within the Rapanui and close to the exposed slope surface.

A narrow zone of high shear plastic strain developed from the upper cliff face towards the crest. Most of the lower Mount Messenger material remained at very low plastic strain levels.

The spatial distribution of the maximum shear plastic strain broadly corresponded with the yielded-element distribution, with both results showing that the largest response at the critical stage occurred within the upper part of the cliff.

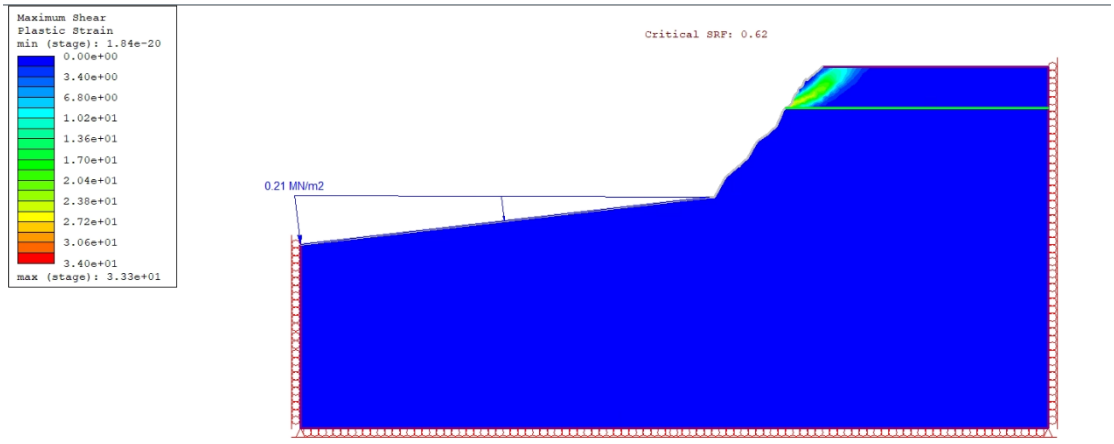


Figure 21: Maximum shear plastic strain distribution at the critical SRF of 0.62 for Scenario

5.4 Scenario 3

5.4.1 Scenario 3 (weekly averaged rainfall)

The analysis using the weekly averaged rainfall input returned a critical SRF of 0.49. The total head distribution at the critical stage is shown in figure 22. The groundwater flow vectors were concentrated mainly within the Rapanui formation and near the exposed cliff face, with the arrows showing flow towards the slope surface.

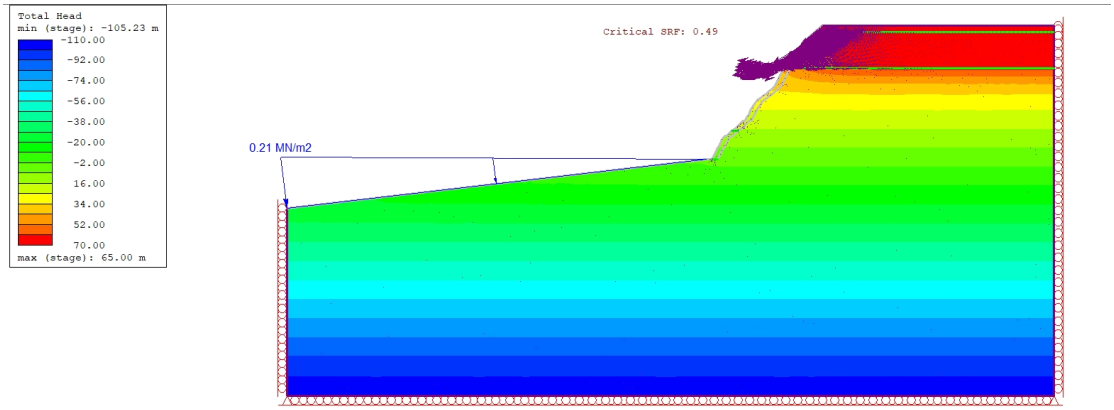


Figure 22: Total head distribution and groundwater flow directions under the weekly averaged rainfall condition at the critical SRF of 0.49

The distribution of yielded elements at the same critical stage is presented in figure 23. A large yielded zone developed within the Rapanui formation. Most of the yielded material was located at the top of the cliff. In contrast, most of the deeper Mount Messenger material remained unyielded.

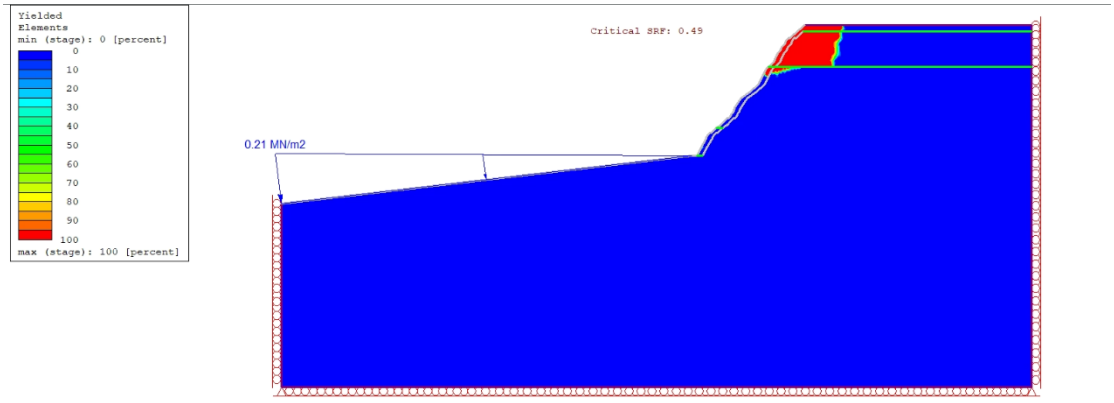


Figure 23: Distribution of yielded elements under the weekly averaged rainfall condition at the critical SRF of 0.49

The corresponding maximum shear plastic strain distribution is shown in figure 24. The maximum shear plastic strain reached approximately 50.5 at the critical stage. The highest strain values were concentrated within the upper Rapanui formation. A relatively narrow zone of elevated plastic strain extended from the upper cliff face towards the crest. Most of the lower Mount Messenger formation remained at very low plastic strain levels.

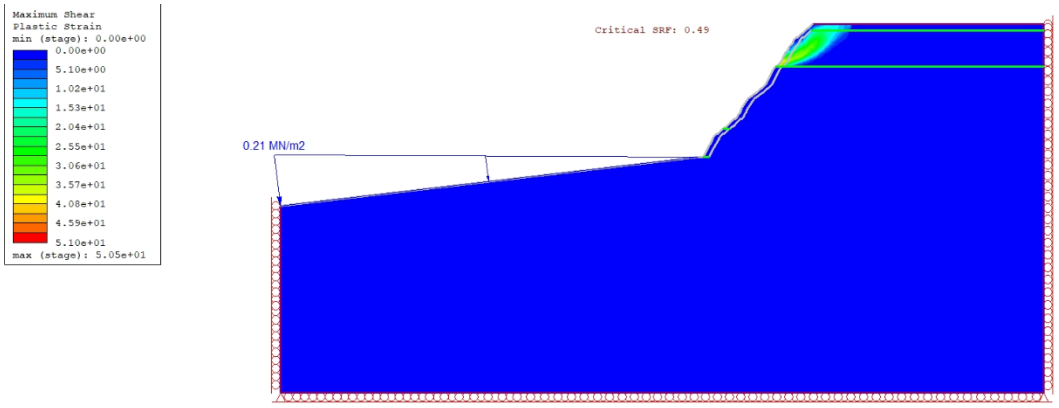


Figure 24: Maximum shear plastic strain distribution under the weekly averaged rainfall condition at the critical SRF of 0.49

5.4.2 Scenario 3 (daily actual rainfall)

The analysis using the actual daily rainfall sequence returned a critical SRF of 0.50. The total head distribution at the critical stage is shown in figure 25.

The groundwater flow vectors were concentrated mainly within the Rapanui formation and near the exposed cliff face, with the arrows showing flow towards the slope surface.

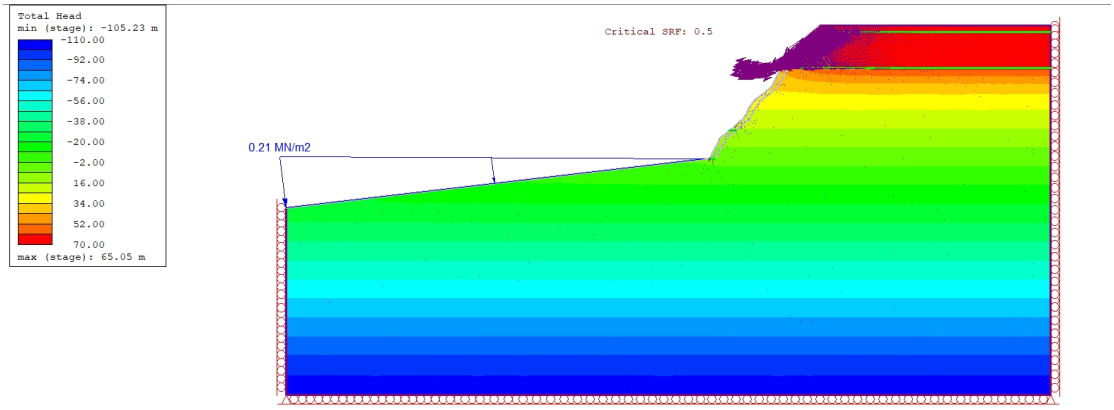


Figure 25: Total head distribution and groundwater flow directions under the daily rainfall condition at the critical SRF of 0.50

The distribution of yielded elements at the same critical stage is presented in figure 26.

A large yielded zone developed within the Rapanui formation. Most of the yielded material was located at the top of the cliff. In contrast, most of the lower Mount Messenger formation remained unyielded.

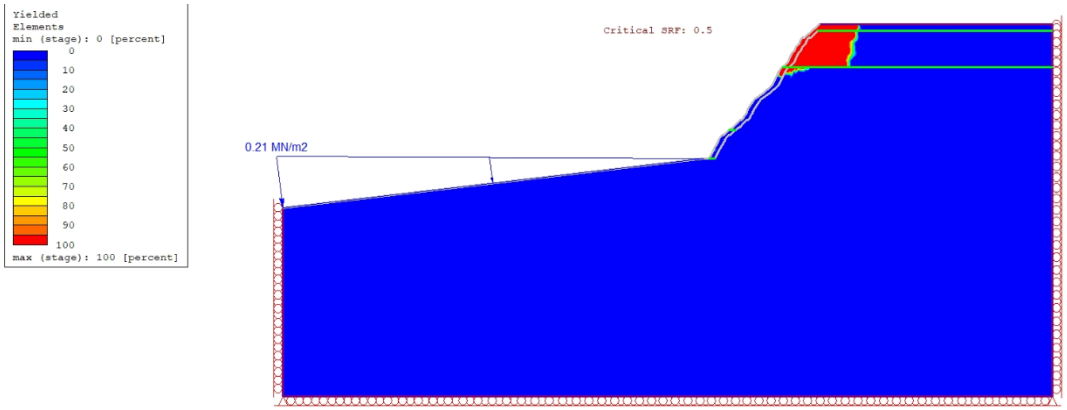


Figure 26: Distribution of yielded elements under the daily rainfall condition at the critical SRF of 0.50

The corresponding maximum shear plastic strain distribution is shown in figure 27.

The maximum shear plastic strain reached approximately 55 at the critical stage. The highest strain values were concentrated within the Rapanui formation, close to the exposed slope surface and above the main material boundary. A relatively narrow zone of elevated plastic strain extended from the upper cliff face towards the crest.

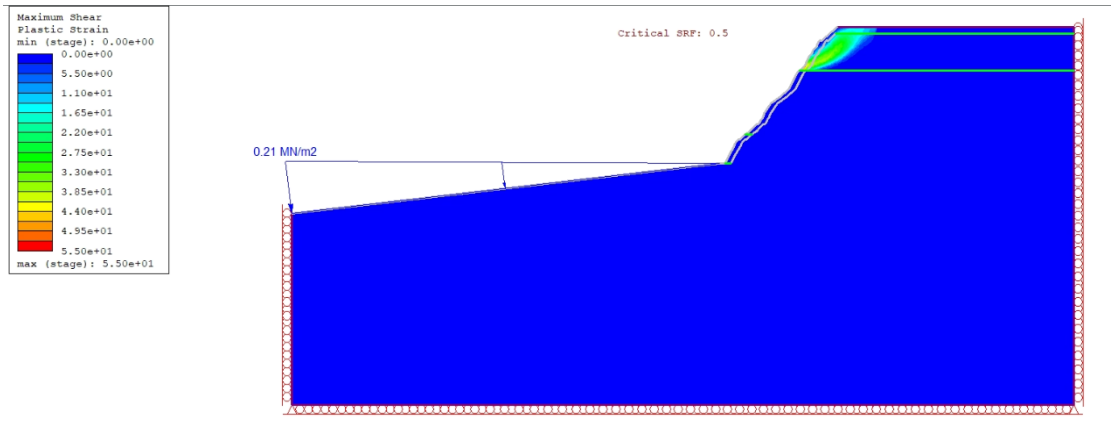


Figure 27: Maximum shear plastic strain distribution under the daily rainfall condition at the critical SRF of 0.50

5.5 Scenario 4

5.5.1 Results under the Dry Condition

The maximum shear plastic strain distribution under the dry condition is shown in figure 28. The maximum shear plastic strain reached approximately 0.985. The highest strain values were also concentrated within the Rapanui formation.

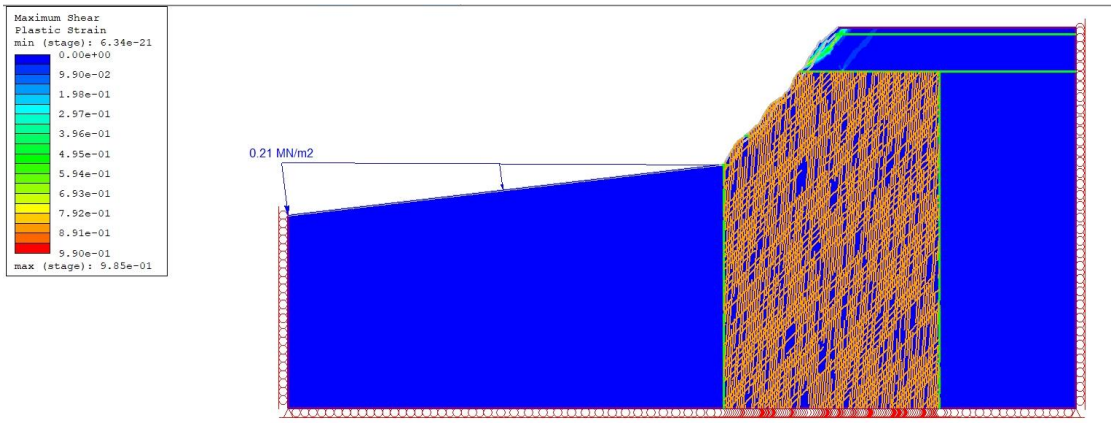


Figure 28: Maximum shear plastic strain distribution under the dry condition for Scenario 4

The distribution of yielded joints within the Mount Messenger formation is shown in figure 29. Yielded joints, marked in red, were mainly observed within the near-surface part of the jointed region. This highlights the instability process in Mount Messenger formation due to the structural condition of the rock mass.

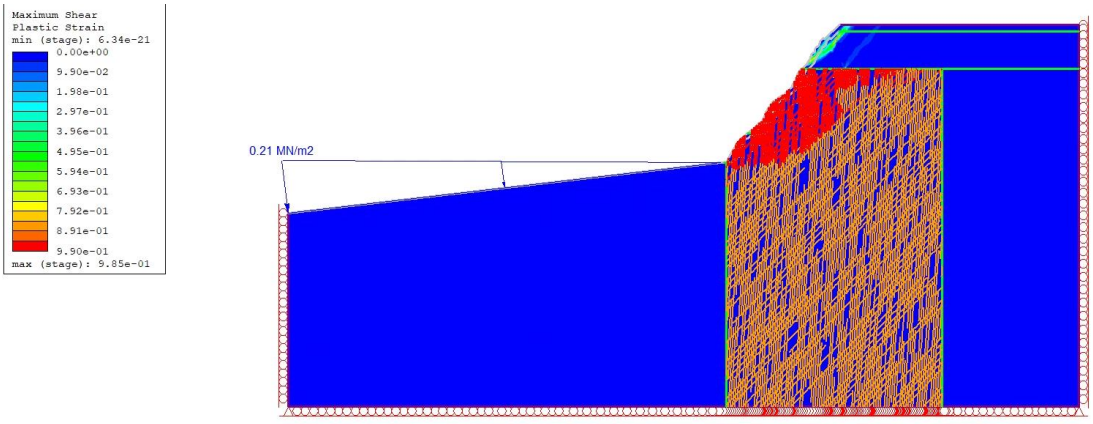


Figure 29: Distribution of yielded joints within the jointed Mount Messenger Formation under the dry condition

The normal and shear displacements recorded along the yielded joints are presented in figure 30 and 31.

The light brown line in the figure represents the degree of normal displacement. From which it can be found that the normal displacement is observed all along the yielded joints close to surface. Among all yielded joints, the maximum normal displacement is observed at around 9 meters to cliff toe. The maximum normal displacement is -0.291 meters, the negative value represents the opening.

The corresponding shear displacement was approximately −0.174 m. The largest joint movements shown in the model were concentrated close to the exposed lower cliff, while smaller movements were observed farther into the jointed rock mass.

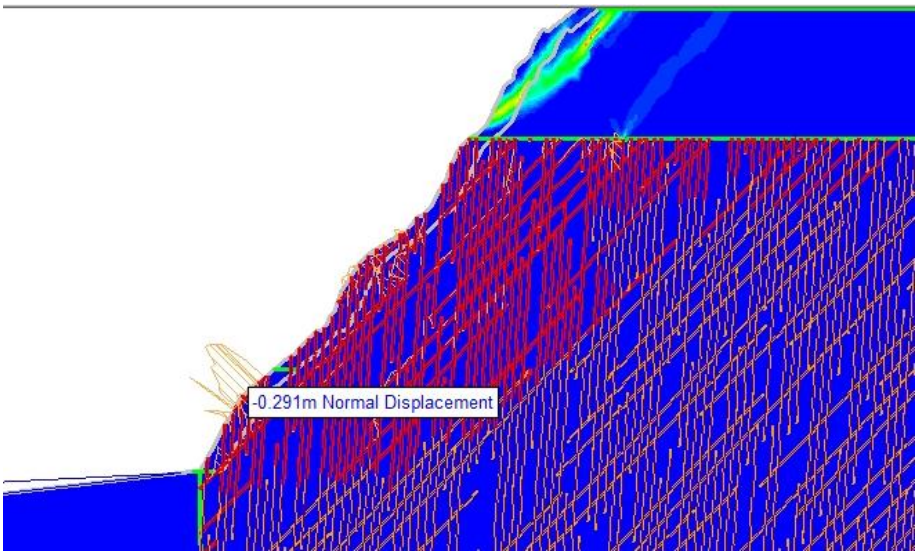


Figure 30: normal displacement along yielded joints under the dry condition (scenario 4)

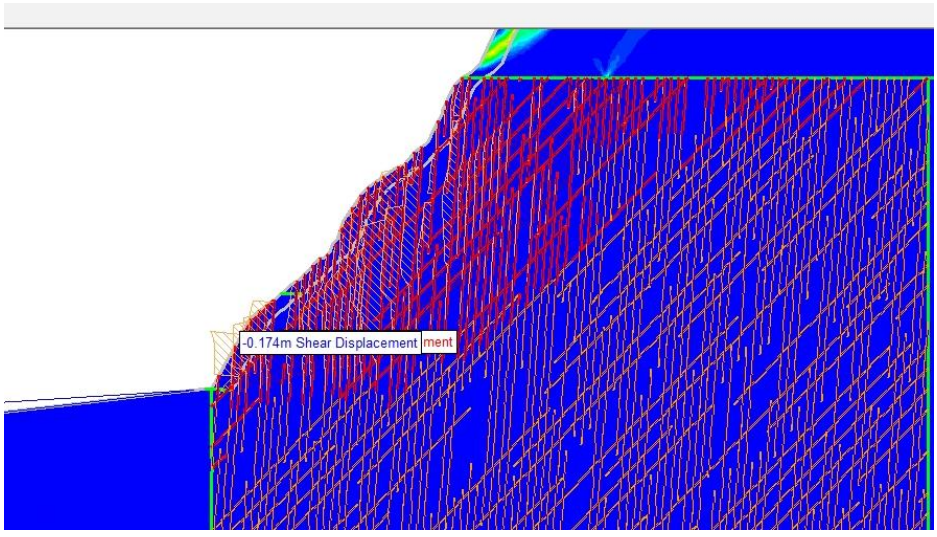


Figure 31: shear displacement along yielded joints under the dry condition (scenario 4)

5.5.2 Results under Weekly Averaged Rainfall

The maximum shear plastic strain distribution under the weekly averaged rainfall condition is shown in figure 32. The maximum shear plastic strain reached approximately 63.4. The highest strain values were again concentrated within the upper part of the cliff, with elevated strain extending from the exposed slope towards the crest.

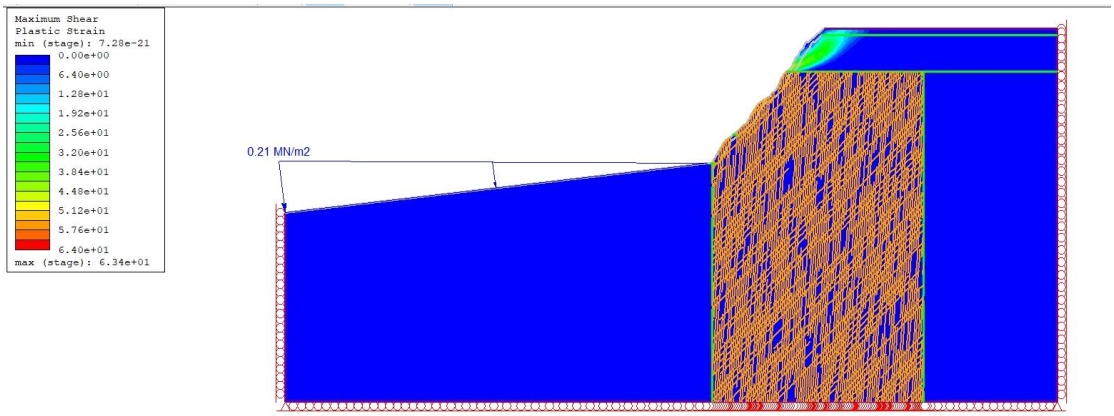


Figure 32: Maximum shear plastic strain distribution under the weekly averaged rainfall condition for Scenario 4.

The normal displacement along selected yielded joints is shown in figure 33.

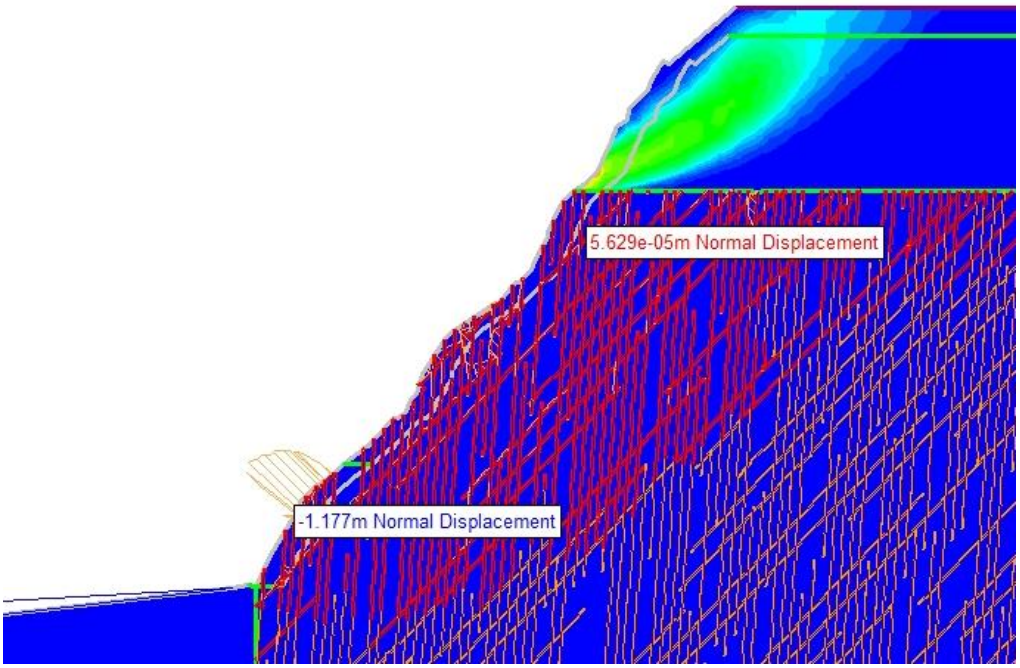


Figure 33: Normal displacement among yielded joints under the weekly averaged rainfall condition

Yielded discontinuities were also observed throughout the jointed part of the Mount Messenger Formation, particularly towards the exposed cliff face. A yielded joint located close to the lower exposed slope recorded a normal displacement of approximately −1.177 m. In comparison, a joint close to the upper boundary of the jointed region showed only a very small normal displacement of approximately 5.63×10^{-5} m. The larger normal joint displacement was therefore concentrated within the lower part of the exposed cliff.

The corresponding shear displacement is shown in figure 34.

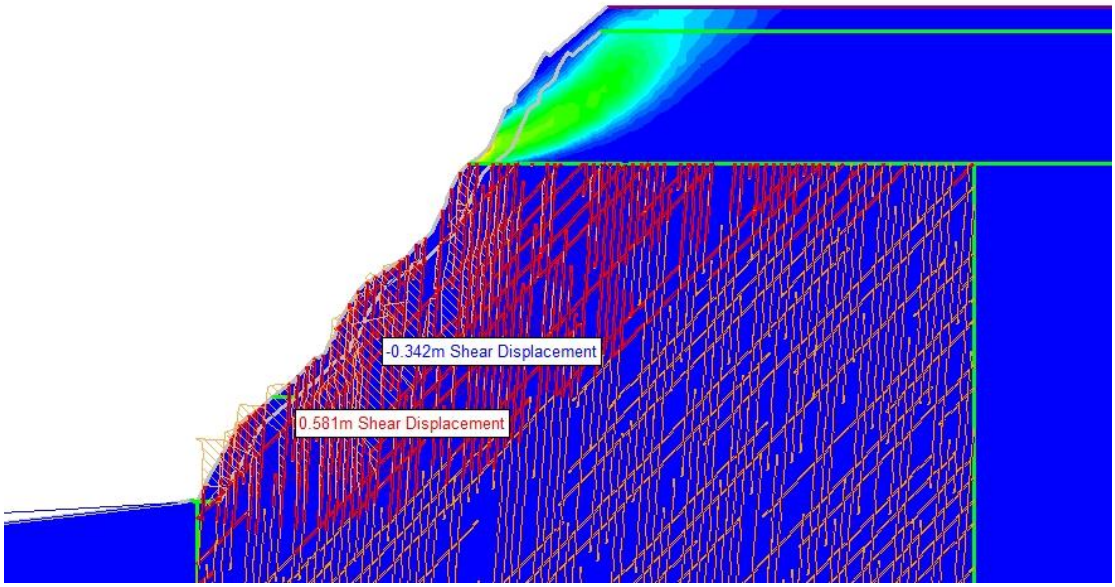


Figure 34: Shear displacement among yielded joints under the weekly averaged rainfall condition

Shear displacement varied between the yielded discontinuities. Values of approximately 0.581 m and −0.342 m were recorded at selected joints within the lower cliff. The positive and negative values represent displacement in opposite directions relative to the defined joint shear direction. The larger shear movements were concentrated within the near-surface part of the jointed rock mass.

6. Discussion and Conclusion

6.1 Overview

This study investigated the stability of a layered coastal rock slope using numerical analyses, with particular attention to rainfall, weathering, wave-action-induced mechanical degradation, and rock discontinuities. Different modelling approaches were used to examine both the global stability of the slope and the local behavior of the lower

jointed rock mass.

The results show that the process of instability affecting the cliff are different according to the characteristics of the two rock formations. While the Rapanui formation rock mass behaves as a weak continuum material in which the discontinuities cannot be clearly identified, the Mount Messenger rock mass is a classical discontinuum medium, where the instability processes are clearly controlled by the characteristics of the discontinuities. The upper part of the slope is mainly controlled by rainfall and weathering, while the lower part is more strongly influenced by wave-related mechanical degradation and discontinuity-controlled deformation. Consequently, the numerical modelling has to be considered two different geotechnical models: an equivalent continuum model for Rapanui formation and a discontinuum model for Mount Messenger formation. In this way, numerical analyses can provide a combined interpretation of global instability and local structural damage within the same coastal slope system.

6.2 Main Conclusions

6.2.1 Initial stability and the effect of rainfall

The baseline model gave a factor of safety of 1.08, indicating that the slope had only a limited stability margin even before rainfall and weathering were considered. The slope was therefore already relatively close to a limiting condition under the idealized dry and unweathered state. This is a realistic scenario, as the evidences show that the cliff retreated due to environmental actions like rainfalls and weathering, meaning that it must originally have already been very close to limit equilibrium conditions.

When weekly averaged rainfall was introduced, the factor of safety decreased to 0.62, being the instability confined to the Rapanui formation if the discontinuum character of the Mont Messenger formation was not taken into account. This represents a reduction of approximately 42.6% from the baseline condition and was the largest change among the directly comparable cases.

6.2.2 Combined influence of rainfall and weathering

When weathering was considered together with weekly averaged rainfall, the factor of safety decreased further from 0.62 to 0.49. This shows that weathering increased the vulnerability of the slope to rainfall-induced instability.

The comparison between the different cases suggests that rainfall and weathering play different but related roles. Rainfall acts mainly as the triggering factor, while weathering reduces the available resistance of the slope material and makes the slope

more sensitive to rainfall.

The combined effect is particularly important in the upper mudstone, where weaker material properties and hydraulic changes occur together. The results therefore suggest that long-term material degradation can prepare the slope for failure, while rainfall provides the short-term condition that activates or accelerates instability.

6.2.3 Influence of rainfall temporal resolution

Under weathered conditions, the factor of safety was 0.50 for daily rainfall and 0.49 for weekly averaged rainfall. The difference between the two values is very small.

For the conditions simulated in this study, the final global stability was therefore relatively insensitive to whether rainfall was represented using daily or weekly averaged data. This suggests that the final slope condition was more strongly controlled by the material strength than by the temporal resolution of the rainfall input. This limited sensitivity may also be partly attributed to the relatively low rainfall values considered in the simulations, which produced only modest changes in infiltration and pore-water pressure. Under more intense rainfall conditions, the influence of rainfall temporal resolution may become more significant.

6.2.4 Different failure behavior of the two tock formations

In the explicitly jointed model, the critical concentration of shear strains was consistently located within the Rapanui formation.

The stability of the Mount Messenger formation was controlled by the presence of discontinuities set, so it was therefore evaluated using local indicators such as yielded joints, shear displacement, normal displacement, and joint strength mobilization. The Mount Messenger formation was also modelled with degraded mechanical properties to represent the effect of long-term wave action. Under this condition, the rock mass became more susceptible to discontinuity-controlled deformation and local damage.

The numerical results therefore indicate a clear difference between the instability mechanisms of the two parts of the slope. This distinction is important because the absence of a global failure surface in the Mount Messenger formation does not mean that the lower slope is undamaged or fully stable. Local sliding, opening, joint yielding, or block movement may develop, thus becoming predisposing factors for the instability of the upper slope.

6.2.5 Overall failure mechanism

The slope behavior identified in this study is best described as spatially differentiated

and progressive rather than uniform.

The slope starts from a condition of limited stability. Rainfall then acts as the main trigger for global instability of the Rapanui formation, while weathering increases its sensitivity to rainfall-induced weakening.

The lower hard rock follows a different mechanism. Long-term wave action contributes to mechanical degradation, while existing discontinuities control the development of local deformation. This response is reflected more clearly by joint yielding and displacement than by the global factor of safety.

The overall mechanism can therefore be summarized as follows:

limited initial stability → rainfall-induced weakening → weathering-amplified response in the upper mudstone → global instability, together with wave-related degradation and discontinuity-controlled local damage in the lower rock mass.

The main implication is that the slope should not be treated as a homogeneous system controlled by one single process. Instead, different parts of the slope respond to different environmental and geological controls, and both global and local behavior need to be considered when interpreting long-term stability.

6.3 Implications

The results suggest that the upper mudstone should be treated as the main area of concern for global slope stability. Since rainfall has a strong influence on the calculated factor of safety, monitoring should pay particular attention to rainfall, pore-water pressure, groundwater response, and deformation within the upper slope.

Drainage and the control of rainfall infiltration are therefore likely to be important for slope management. However, specific drainage measures were not tested directly in this study, and their effectiveness should be evaluated separately before being adopted in engineering design.

The lower slope requires a different type of assessment. Wave-related degradation and joint activity may still lead to local block loosening, falling, tilting, sliding, or opening. Monitoring of the lower slope should therefore focus on joint condition, local displacement, and visible deterioration in the wave-exposed zone.

A further implication is that a single global factor of safety is not sufficient for this type of layered coastal slope. Global stability and local structural damage should be considered together, as weak upper materials and jointed lower rock behaves differently under the same environmental processes.

6.4 Limitations of the Study

Several limitations should be considered when interpreting the numerical results.

First, the analyses were carried out in two dimensions. The model therefore cannot fully represent three-dimensional slope geometry, lateral confinement, discontinuity persistence, or three-dimensional groundwater flow.

Second, the mechanical and hydraulic properties used in the model are representative values. Natural variation in rock strength, stiffness, permeability, and joint condition introduces uncertainty into the calculated response.

Third, weathering was represented through changes in material properties rather than through a time-dependent weathering process. The model therefore reflects the mechanical condition of weathered material but does not reproduce the complete evolution of weathering.

Fourth, the rainfall boundary conditions are simplified representations of real rainfall. Although daily rainfall contains more temporal detail than weekly averaged rainfall, short-duration rainfall peaks, evaporation, runoff, and antecedent moisture conditions are not fully represented.

Finally, wave action was represented through mechanical property degradation rather than direct dynamic loading. The model therefore does not explicitly simulate wave impact, cyclic loading, transient water pressure, or progressive toe erosion.

6.5 Recommendations for Future Research

Future work should include more field data for model calibration, particularly rainfall, groundwater level, pore-water pressure, and slope displacement. These data would provide a stronger basis for comparing the numerical response with actual slope behavior.

Further rainfall scenarios should also be considered, including short-duration high-intensity rainfall, long-duration rainfall, and different antecedent moisture conditions. This would help clarify whether rainfall intensity, duration, or cumulative infiltration has the greatest influence on slope response.

Sensitivity analysis of the main mechanical and hydraulic parameters would also be useful, especially for cohesion, friction angle, stiffness, permeability, and joint strength, in particular when there is very little information, like in the study case.

For the lower slope, future modelling should compare undegraded and different levels of wave-degraded rock directly. This would allow the effect of wave-action-induced

mechanical degradation to be quantified more clearly. The influence of mechanical degradation and toe erosion could also be investigated separately.

Where sufficient geological data are available, three-dimensional modelling and more detailed discontinuity representation could be used to improve the understanding of local block behavior and the interaction between the upper and lower parts of the slope.

Reference list:

Adams, P.N., Storlazzi, C.D. and Anderson, R.S. (2005). Nearshore wave-induced cyclical flexing of sea cliffs. *Journal of Geophysical Research: Earth Surface*, 110(2), F02002. doi:10.1029/2004JF000217.

Duperret, A., Taibi, S., Mortimore, R.N. and Daigneault, M. (2005). Effect of groundwater and sea weathering cycles on the strength of chalk rock from unstable coastal cliffs of NW France. *Engineering Geology*, 78(3–4), pp.321–343. doi:10.1016/j.enggeo.2005.01.004.

Earlie, C., Masselink, G. and Russell, P. (2018). The role of beach morphology on coastal cliff erosion under extreme waves. *Earth Surface Processes and Landforms*, 43(6), pp.1213–1228. doi:10.1002/esp.4308.

Fazio, N.L., Perrotti, M., Andriani, G.F., Mancini, F., Rossi, P., Castagnetti, C. and Lollino, P. (2019). A new methodological approach to assess the stability of discontinuous rocky cliffs using in-situ surveys supported by UAV-based techniques and 3-D finite element model: a case study. *Engineering Geology*, 260, Article 105205. doi:10.1016/j.enggeo.2019.105205.

Genchi, S.A., Vitale, A.J. and Perillo, G.M.E. (2025). Coastal cliff erosion: a bibliometric analysis and literature review. *Anthropocene Coasts*, 8, Article 8. doi:10.1007/s44218-025-00072-2.

Guo, P., Gu, J., Su, Y., Wang, J. and Ding, Z. (2021). Effect of cyclic wetting–drying on tensile mechanical behavior and microstructure of clay-bearing sandstone. *International Journal of Coal Science & Technology*, 8, pp.956–968.

Hawkins, A.B. and McConnell, B.J. (1992). Sensitivity of sandstone strength and deformability to changes in moisture content. *Quarterly Journal of Engineering Geology*, 25(2), pp.115–130. doi:10.1144/GSL.QJEG.1992.025.02.05.

Hua, W., Dong, S., Li, Y., Xu, J. and Wang, Q. (2015). The influence of cyclic wetting and drying on the fracture toughness of sandstone. *International Journal of Rock Mechanics and Mining Sciences*, 78, pp.331–335. doi:10.1016/j.ijrmms.2015.06.010.

Huang, S., Wang, J., Qiu, Z. and Kang, K. (2018). Effects of cyclic wetting-drying conditions on elastic modulus and compressive strength of sandstone and mudstone. *Processes*, 6(12), Article 234. doi:10.3390/pr6120234.

Lawrence, J.A., Mortimore, R.N., Stone, K.J. and Busby, J.P. (2013). Sea saltwater weakening of chalk and the impact on cliff instability. *Geomorphology*, 191, pp.14–22. doi:10.1016/j.geomorph.2013.02.022.

Lawrence, J.A., Spence, R., Mortimore, R.N., Eade, M. and Bottrell, S.H. (2018). Coastal cliff rock mass weakening of Chalk and the impact of salt water. *Proceedings of the Institution of Civil Engineers – Geotechnical Engineering*, 171(6), pp.545–555. doi:10.1680/jgeen.18.00040.

López-Fernández, C., Domínguez-Cuesta, M.J., González-Pumariega, P., Ballesteros, D., Suárez Suárez, L. and Jiménez-Sánchez, M. (2022). Instability mechanisms and evolution of a rocky cliff on the Atlantic coast of Spain. *Journal of Coastal Conservation*, 26, Article 60. doi:10.1007/s11852-022-00907-x.

Napoli, M.L., Barbero, M., Mascioli, F. and Miccadei, E. (2025). Gravity-induced collapse of a soft rock cliff due to notch growth. *Environmental Geotechnics*, 12(3), pp.183–193. doi:10.1680/jenge.24.00052.

Naylor, L.A., Stephenson, W.J. and Trenhaile, A.S. (2010). Rock coast geomorphology: recent advances and future research directions. *Geomorphology*, 114(1–2), pp.3–11. doi:10.1016/j.geomorph.2009.02.004.

Naylor, L.A., Coombes, M.A. and Viles, H.A. (2012). Reconceptualising the role of organisms in the erosion of rock coasts: a new model. *Geomorphology*, 157–158, pp.17–30. doi:10.1016/j.geomorph.2011.07.015.

Rosser, N.J., Brain, M.J., Petley, D.N., Lim, M. and Norman, E.C. (2013). Coastline retreat via progressive failure of rocky coastal cliffs. *Geology*, 41(8), pp.939–942. doi:10.1130/G34371.1.

Scrivano, S. and Gaggero, L. (2020). An experimental investigation into the salt-weathering susceptibility of building limestones. *Rock Mechanics and Rock Engineering*, 53, pp.5329–5343. doi:10.1007/s00603-020-02208-x.

Steiger, M. (2005). Crystal growth in porous materials—I: the crystallization pressure of large crystals. *Journal of Crystal Growth*, 282(3–4), pp.455–469. doi:10.1016/j.jcrysgro.2005.05.007.

Sunamura, T. (1992). *Geomorphology of Rocky Coasts*. Chichester: John Wiley & Sons.

Sunamura, T. (2015). Rocky coast processes: with special reference to the recession of soft rock cliffs. *Proceedings of the Japan Academy, Series B*, 91(9), pp.481–500. doi:10.2183/pjab.91.481.

Trenhaile, A.S. (2002). Rock coasts, with particular emphasis on shore platforms. *Geomorphology*, 48(1–3), pp.7–22. doi:10.1016/S0169-555X(02)00173-3.

Vásárhelyi, B. and Ván, P. (2006). Influence of water content on the strength of rock.

Engineering Geology, 84(1–2), pp.70–74. doi:10.1016/j.enggeo.2005.11.011.

Young, A.P., Guza, R.T., Flick, R.E., O'Reilly, W.C. and Gutierrez, R. (2009). Rain, waves, and short-term evolution of composite seacliffs in southern California. *Marine Geology*, 267(1–2), pp.1–7. doi:10.1016/j.margeo.2009.08.008.

Young, A.P., Guza, R.T., Matsumoto, H., Merrifield, M.A., O'Reilly, W.C. and Swirad, Z.M. (2021). Three years of weekly observations of coastal cliff erosion by waves and rainfall. *Geomorphology*, 375, Article 107545. doi:10.1016/j.geomorph.2020.107545.

Yu, S. and Oguchi, C.T. (2010). Role of pore size distribution in salt uptake, damage, and predicting salt susceptibility of eight types of Japanese building stones. *Engineering Geology*, 115(3–4), pp.226–236. doi:10.1016/j.enggeo.2009.05.007.

Zhao, Z., Yang, J., Zhou, D. and Chen, Y. (2017). Experimental investigation on the wetting-induced weakening of sandstone joints. *Engineering Geology*, 225, pp.61–67. doi:10.1016/j.enggeo.2017.04.008.

Zhao, Z., Yang, J., Zhang, D. and Peng, H. (2017). Effects of wetting and cyclic wetting–drying on tensile strength of sandstone with a low clay mineral content. *Rock Mechanics and Rock Engineering*, 50(2), pp.485–491. doi:10.1007/s00603-016-1087-9.